WHEN CONTEXT CHANGES: UNDERSTANDING UPDATE FAILURES IN LLMS

Junyu Guo junyuguo24@berkeley.edu
Yuchen Fang yc_fang@berkeley.edu
Shangding Gu shangding.gu@berkeley.edu
Costas Spanos spanos@eecs.berkeley.edu
James Demmel demmel@berkeley.edu
Javad Lavaei lavaei@berkeley.edu
University of California, Berkeley

github.com/JamesJunyuGuo/CICM

arXiv:2609.38866v2 [cs.AI] 29 Oct 2026

ABSTRACT

As preferences, goals, and facts change, LLM agents must use the current state while earlier versions remain in context. Yet they can answer with an old value of the same variable, a failure that we call **stale binding**. To study when models use outdated information and why, we introduce Controlled In-Context Memory (CICM), a benchmark for tracking and using updated information in conversations and agent logs. We observe that even frontier reasoning models can fail to recover the current state. We find that in open-source models probes can still recover the updated value when the model answers with an old one, pointing to a failure to select information that remains available. Component tests in Qwen and Pythia identify a mechanism for this selection failure: attention drift, where attention favors old values over the current one when producing an answer. We study a one-layer transformer to mathematically understand how this phenomenon happens: when attention scores are similar, several old values can together receive more attention than the current value. Guided by this explanation, we redirect attention toward the current value without further training. When the current value is requested directly, adjusting this intervention for each input corrects most old-value errors across various model families while preserving nearly all initially correct answers. Reliable context management therefore requires more than remembering updated information: models must use it to guide their answers.

1 INTRODUCTION

LLM agents operate in dynamic environments where context continuously evolves. During an interaction, users revise preferences, switch objectives, and update facts that guide future actions, such as an address or a project deadline. A planning agent must follow the revised goal, and a coding agent must use the current requirements. However, earlier versions remain in the conversation or execution log alongside their updates. Reliable context management therefore requires identifying which state is currently valid and using it to guide the next response.

Prior work examines context management through retrieval, memory, and forgetting. Long-context studies test information access at different positions (Liu et al., 2024); conversational benchmarks evaluate remembering facts, tracking updates, and following preferences (Wu et al., 2025a; Zhao et al., 2025). ICF-Bench tests selective forgetting of information that should no longer guide a response (Qian et al., 2026), while interference studies show that repeated updates to the same key impair recall (Wang & Sun, 2025; Chattaraj & Raj, 2026). These findings motivate a closer diagnosis of update errors: what information does a wrong answer use, and why does it win over the current state? We investigate this question by giving models successive updates to the same variable and asking for its current value, with the full history available. For example, if a meal preference changes from gluten-free to Mediterranean, answering *gluten-free* returns an old value of the right variable; answering a music preference confuses variables. We call the former error *stale binding*. In controlled experiments, repeated updates predominantly produce old-value errors even when equally long contexts without updates remain easy. The problem also reaches complex operational histories:

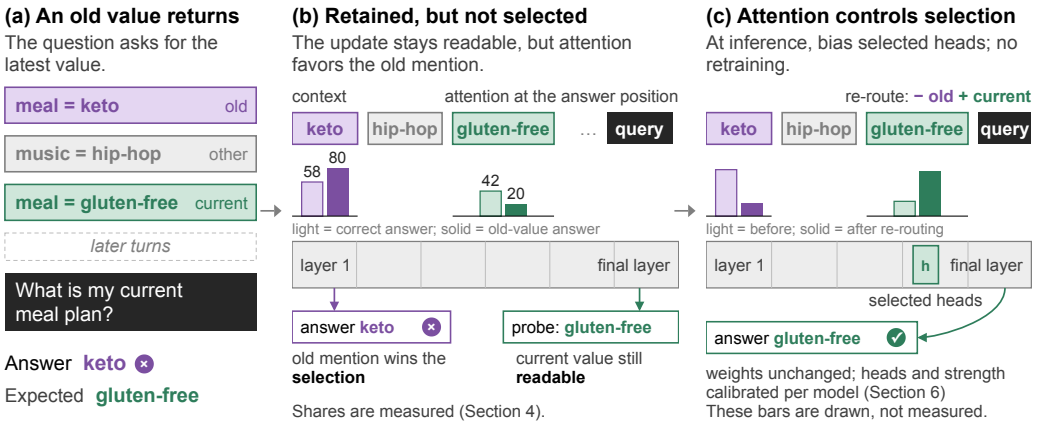

Retaining an update does not guarantee using it; attention can control selection.

Figure 1: **a–b**, An old value can win while the current value remains readable. The bars in **b** are measured attention shares at the answer position (Section 4). **c**, Redirecting attention can correct selection without retraining.

GPT-5.6 Sol and Claude Opus 4.8 produce incorrect current-state answers after completing their reasoning, while answering every paired current-state snapshot correctly.

We ask how these errors arise, whether the current information remains available inside the model, and whether changing how it is selected can repair the answer. To connect these questions, we introduce *Controlled In-Context Memory (CICM)*, a benchmark with programmatic state labels and error categories that support systematic diagnosis beyond accuracy. Its preference core builds on PrefEval content and supports probes and interventions. It also includes new dialogues, decisions under changing constraints, and operational logs extend the same update problem to richer tasks. This design allows us to connect behavioral errors to internal measurements, a simple mathematical explanation, and targeted interventions (Figure 1).

Overall, our contributions can be summarized as follows:

1. **A diagnostic benchmark for in-context updates.** CICM distinguishes old-value reuse from other-variable confusion across dialogue and agent-log tasks, connecting controlled mechanism tests with complex histories that challenge frontier models.
2. **Selection failures and attention drift.** Probes recover current values even when old ones are chosen. Measurements and component interventions in various model families identify *attention drift*: attention favors old values over the current one, affecting which value reaches the answer.
3. **A one-layer transformer explanation.** We show how position shapes attention scores and how several old values can together receive more attention than the current value, making the competition behind selection explicit.
4. **Training-free repair at test time.** Redirecting attention improves direct current-value answers across Qwen, Llama, Mistral, and Gemma without changing model weights. Adjusting the intervention for each input corrects most old-value errors while preserving nearly all initially correct answers.

2 The Stale-Binding Phenomenon

A binding pairs a variable with a value. When context assigns the same variable more than once, the latest explicit assignment gives its current value while earlier ones remain as old values, still visible to the model. An *old-value error*, or *stale binding*, returns an old value of the queried variable instead of its current one. We first isolate this error using synthetic overwrite tasks, and then examine richer dialogue and operational updates. Answers are classified as current, old, another variable's value, or others. Section 3 introduces CICM's construction. We begin with a simple overwrite task: a

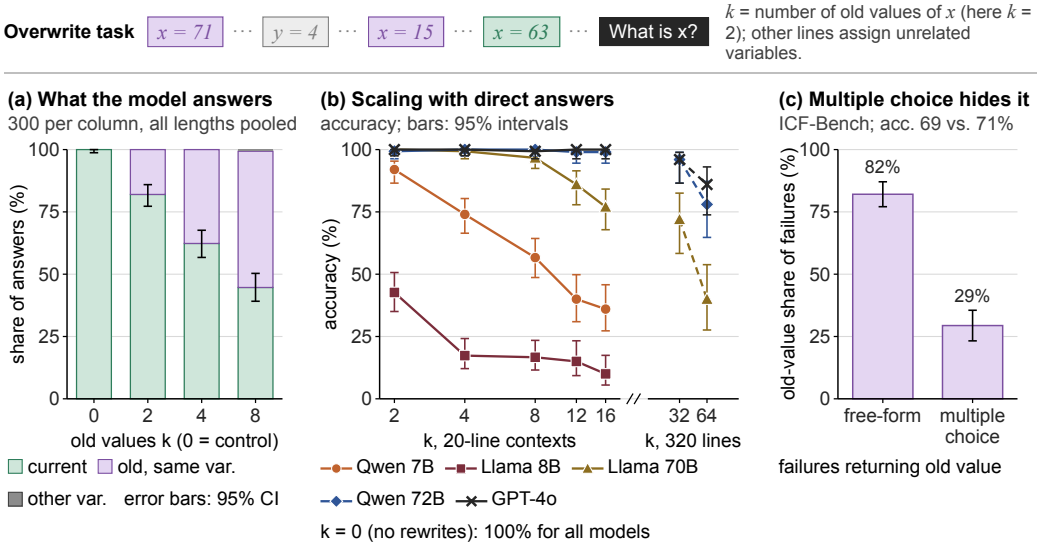

Figure 2: Old values, not length alone. **a**, Repeated updates mainly produce old-value errors; longer contexts amplify the effect. **b**, Old-value errors persist at $k = 64$ with direct answers. **c**, Multiple choice masks old-value retrieval on ICF-Bench at similar accuracy. Bars: 95% intervals; sample sizes and estimation in Appendices C.1 and B.4.

target variable is repeatedly reassigned while unrelated lines control context length. Qwen2.5-7B remains nearly perfect without overwrites, but accuracy declines as more old values compete with the current one at matched lengths (Figure 2a). Among 333 failures, 331 return an old value of the queried variable; two copy another in-context value, and none introduces an absent value. The most recent old value is overrepresented relative to a uniform choice among old values at $k = 2, 4, 8$ (Appendix B.2), here k refers to the number of the old values. Also, a parallel-variable control shows negligible cross-variable leakage. (Appendix C.1).

Scale postpones the failure without changing its nature. 70B-class models and GPT-4o tolerate more revisions but still fail at $k = 64$, while every matched 320-line prompt without overwrites is answered correctly (Figure 2b): the difficulty comes from the updates, not from the context length. The error also keeps its signature. Qwen2.5-72B and GPT-4o return old values on every error, Llama-3.1-70B shows a more varied mixture, and recent old values are again favored, as all seven GPT-4o errors select one of the two most recent (Appendix B.2). Spending more computation at answer time does not remove it either. On paired 80-line prompts, a larger direct-answer budget alone leaves Qwen's overwrite accuracy unchanged, whereas concise reasoning improves it; every remaining error still returns an old value (Appendix F.2). That benefit does not survive load: at $k = 256$, GPT-4o returns old values on 32 of 36 prompts even with concise reasoning, although GPT-5 and Gemini answer all 36 correctly (Appendix Table 16).

Frontier failures under complex updates. The error survives into frontier models once the update structure grows complex. In 2,048-operation warehouse and build-release logs, with complete histories and explicit rules, GPT-5.6 Sol answers 9/40 current-state queries correctly and Opus 4.8 18/40 (18 of 31 completed responses; nine more reach the output cap). Both answer all 40 paired snapshots correctly, so the difficulty is reconstructing the state through the history, not reading it. In an exploratory, pre-specified 17-scenario prefix whose operations take effect only when a later line confirms them, Opus scores 12/17, against 16/17 on a control with the same operations at the same line numbers but each effect stated where it happens. Appendix F.5 gives settings, paired outcomes, and verified examples.

Apart from the scaling results, the answer format decides whether the error is visible. On ICF-Bench Dynamic Preference, Qwen2.5-7B reaches nearly the same accuracy in both formats, yet 82.1% of its free-form failures return an old preference against 29.4% under multiple choice (Figure 2c): supplying options masks old-value retrieval rather than preventing it. Accuracy alone therefore cannot

reveal what a model does with an update. These tasks need a diagnostic benchmark that labels which value a response reused, not only whether it was correct. Motivated by this observation, in Section 3 we will introduce the diagnostic benchmark that we have built for measuring LLMs' in-context update behavior. Appendix Table 5 and Appendix B.4 give the comparison and its scoring.

3 CICM: A Benchmark for In-Context Updates

In this section, we propose CICM as a comprehensive and diagnostic benchmark to test whether models use the current state while earlier versions remain in context. In this benchmark, by setting explicit update rules and programmatic ground truth, we can precisely diagnose which information an incorrect answer reuses (Figure 3). CICM's core components can be summarized as follows.

Dialogue updates. The core uses PrefEval content (Zhao et al., 2025) in 1,200 dialogues about meal, music, and learning preferences. A generator controls values, update order, and competing mentions; language models provide wording. Annotated positions support probes and interventions. Another 180 pilot ledgers span six domains, with single-value, partial-record, and full-record updates.

Decisions and operational state. In 24 procurement and scheduling scenarios, revised constraints determine a unique optimal action. Forty primary operational histories require tracking slot contents through 2,048 dependent handoffs over 16 slots. A deferred variant adds operations that execute only on later confirmation. Paired snapshots supply the resolved state while preserving the query.

Construction and scoring. Answers are fixed before evaluation and checked through span validation, independent state replay, or action enumeration. Direct-value scoring distinguishes current, old, other-variable, and other answers; decision scoring measures optimality and constraint satisfaction. Response availability is recorded separately. Appendix D details construction and provenance; Appendix E gives mixed-answer scoring checks.

3.1 Dialogue validity and decision outcomes

The original preference core adds an ambiguous old-value re-mention in its near condition. Paired follow-ups clarify wording and isolate placement: with identical messages and mention counts, moving an explicitly historical mention nearer the query raises Qwen's old-value rate from 14.8% to 36.7%; GPT-4o returns no old values in either condition (Appendix F.1). On the decision component,

(a) Updating a preference

Dialogue excerpts

"I think **visual** works best for me overall."

"I actually prefer **reading** when I'm trying to understand something new."

[Other turns and preference updates omitted.]

"For the record, **visual** was an earlier choice for my learning style, and is no longer current."

Query (summary)
What is my latest explicitly updated learning style? Later mentions are not updates.

Qwen2.5-7B: visual
Current answer: reading

(b) Tracking a deferred handoff

Agent-log excerpts

```
0876 handoff(
  cycle=[S08,S09,S14,S12]);
branch=production;
status=pending
```

[Intervening log entries omitted.]

```
1007 resolve(seq=0876);
result=committed
```

[Remaining log entries omitted.]

Query (summary)
Which parcel is currently in S14?

Opus 4.8: P7888
Current answer: P7238

Programmatic state check for (b). A pending handoff executes only when committed by a later resolve line. At line 1007, S09 holds P7238; executing the cycle moves it to S14. No later executed operation changes S14. This annotation explains the answer; it was not supplied to the model.

Figure 3: CICM examples. Full cases: Appendices B.1 and F.5.

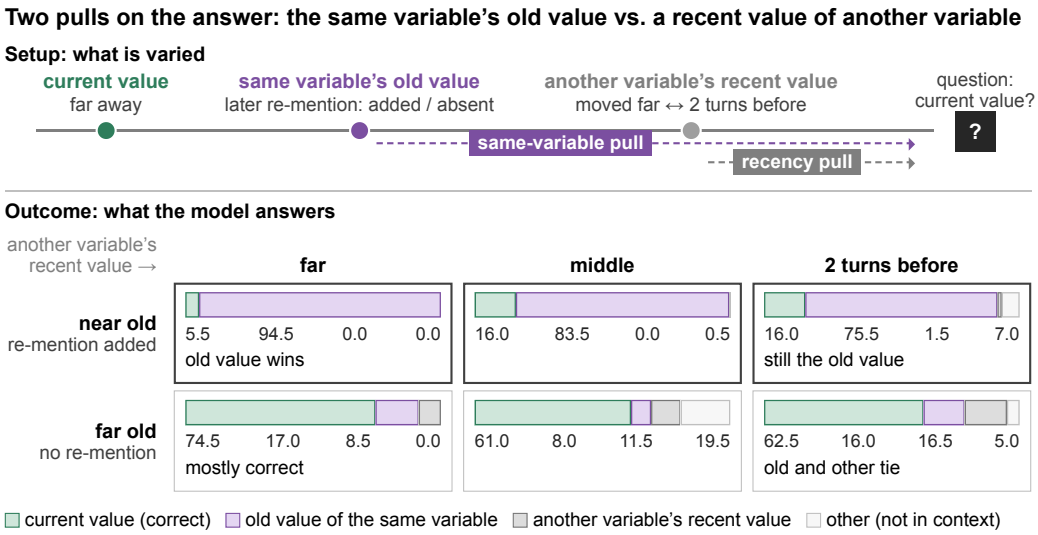

Figure 4: Competing mentions in CICM. Numbers are response percentages.

four reasoning models return optimal actions on 88–95 of 96 full-history prompts; remaining outcomes are invalid outputs, provider failures, or truncations (Appendix F.4).

4 Mechanism Analysis

We ask what the model selects, whether the current value is still available, where attention goes, which components decide, and whether selection can be overridden. Attention drift appears in five models under matched controls, and the tests that open the model up run in Pythia-160M, Qwen2.5-7B and Llama-3.1-8B. Appendix Table 3 records which model supports each claim.

4.1 Identity and Recency Compete

Identity outweighs recency: an old value of the queried variable dominates responses even when another variable was updated more recently. We test this on CICM's preference dialogues with Qwen2.5-7B, querying the current value of one variable. The factorial holds the current assignment far from the query and crosses a later re-mention of the most recent old value (present or absent) with another variable's distance (far, intermediate, or two turns), 200 dialogues per condition (Figure 4).

A nearby re-mention of the old value decides the answer. When the old value is re-mentioned near the query, old-value errors dominate (75.5–94.5%) even though another variable is more recent. Without that re-mention, bringing the other variable close makes old-value and other-variable errors about equally frequent (16.0% and 16.5%). Recency competes only when the old value is not repeated nearby. The re-mention also decides which old value comes back. For $k = 2, 3, 4, 6$, the re-mentioned value accounts for 94.5–100% of old-value answers in both Qwen and Llama. Without it, the most recent old value accounts for 66.7–100% in Qwen and 44.2–61.1% in Llama (Appendix B.2). A re-mention can be read as a renewed preference rather than a repetition. Marking it explicitly historical lowers Qwen's near-source old-value rate to 25.5% without eliminating the errors (Appendix F.1). The original contrast therefore combines wording and mention count with position, and the matched-placement test in Section 3.1 isolates position.

4.2 The Current Value Remains Readable

When a model returns an old value, one possible explanation is that it has lost the current value from its internal representation. However, a linear probe can still recover information about the current value from the model's hidden state, even when its answer is incorrect. On old-value errors, a linear probe assigns the current value a mean probability of 84.8% in Qwen and 82.2% in Llama, against

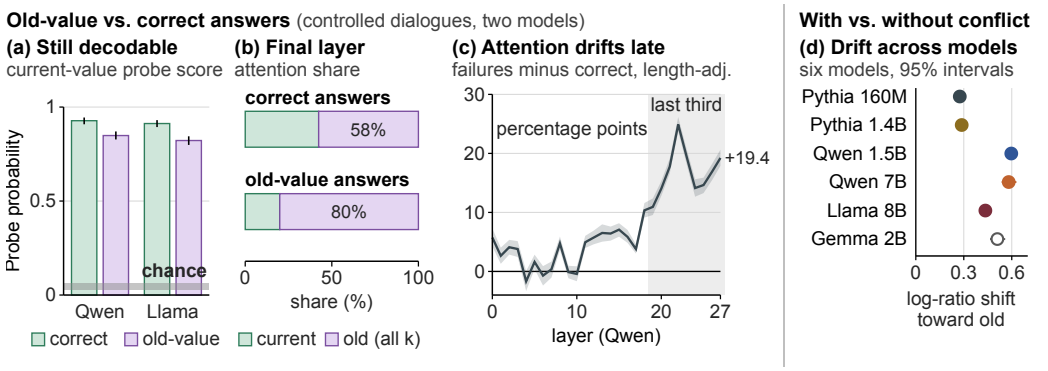

Figure 5: Attention drift: old values take priority. **a**, Mean probe probability assigned to the current value (grey: shuffled labels). **b**, Qwen's final-layer attention favors old values on failures. **c**, In Qwen the length-adjusted failure–correct difference grows in late layers. **d**, Matched conflict–control shifts.

3.2–6.4% when the value labels are randomly reassigned (Figure 5a). Other-variable errors show similar recoverability (Appendix Table 6). The probe reads the standardized final-layer hidden state h_i at the answer position in dialogue i. With learned weights W and bias b, denoted $\phi = (W, b)$, it assigns each of the 21 candidate values v the probability $q_\phi(v \mid h_i) = \mathrm{softmax}(Wh_i + b)_v$. We fit and evaluate it in five folds split by dialogue, so each reported score comes from a probe that did not train on that dialogue. Randomly reassigning the value labels checks whether the scores depend on the true relationship between hidden states and values (Hewitt & Liang, 2019). These are probe probabilities, not answer accuracies.

Readability does fall on failures. After accounting for prompt length, scores on old-value errors are about 7% below those on correct answers in both models. The current value therefore stays accessible to a linear classifier without being used, which is not yet evidence that the model consults it. The next tests examine that selection step, and Appendix C.1 gives the probe details.

4.3 Old values take priority in attention

Attention drift is not specific to one model. We use *attention drift* for attention giving greater priority to old values than to the current value. Comparing each updated dialogue with one of equal token length but no conflicting reassignment, conflicting updates shift attention and query–key matching toward old values in five models with reliable controls, including Llama and answers that are correct (Appendix B.10). Redirecting that attention changes which value is answered in Qwen, Llama and Mistral (Section 6), so the shift is not incidental to the answer. In Qwen, the same measure separates failures from correct answers. For each head at the answer position, let A_{old} and A_{current} be the attention masses summed over old and current assignments, and define the old-value share as

$$\rho_{\text{old}} = \frac{A_{\text{old}}}{A_{\text{old}} + A_{\text{current}}}. \tag{1}$$

Averaged across heads and adjusted for prompt length, the share is 19.4 percentage points higher on failures, with the largest shift in late layers. The matched-context shift and the failure-associated shift measure different contrasts.

4.4 Which components decide the answer

A shift in attention on failures is still a correlation. By replacing components we can causally test whether they produce the answer.

Attention selects positions through query–key matching and transmits their information through value vectors and the output projection (Vaswani et al., 2017). For 120 failed synthetic overwrite prompts, we construct successful counterparts with identical candidate values and positions, renaming earlier assignments to remove competition for the queried variable (Appendix B.6). We then replace components in failed runs with their successful counterparts (Qwen rows in Table 1). Recovery

concentrates in late hidden states and old-value keys, implicating late selection and competing keys. For the current-minus-old answer-score gap g, we measure recovery after replacement as

$$R = 100\,\frac{g_{\text{replaced}} - g_{\text{failed}}}{g_{\text{successful}} - g_{\text{failed}}}. \tag{2}$$

Here $R = 100$ restores the successful gap, and $R < 0$ favors the old value further.

Replacement narrows the error to a pathway rather than to individual heads. Naming them takes exhaustive intervention: removing each head in turn, replacing the inputs to its key and query, and matching every result against layer-matched random controls. Pythia-160M produces the same old-value answers and is small enough to carry that program through. Removing the heads selected to promote old values corrects 38.4% of held-out old-value answers, against 8.7% for layer-matched random sets, with discovery and evaluation on separate examples. The recovery concentrates in the query–key path, where matching favors old assignments while the value pathway keeps transmitting whatever is attended. Replacing selected inputs to a single head's key recovers 75% of the answer-score gap, against 6% for layer-matched random inputs (Table 1). As in the larger models, the current value remains readable on these failures. Appendix B.8 gives the full experimental results.

Table 1: Causal evidence in Qwen-7B and Pythia-160M. Each row specifies its comparison.

Intervention comparison	Result
Answer-score-gap recovery (%)	
Qwen: late / early–middle states	78.1 / −0.5
Qwen: old / current keys	49.2 / −21.3
Pythia key inputs: targeted / random	75 / 6
Old-value errors corrected (%)	
Pythia head removal: targeted / random	38.4 / 8.7

Pythia comparisons are held out, and random sets are matched by layer. Full controls: Appendices B.6 and B.8.

4.5 Selection is decided late

Locating the components is not the same as being able to change what they do, and when the answer is settled matters for both. Repairing the update once does not secure it. In Pythia-160M, replacing the update's attention key with the counterpart from a successful run corrects 92.8% of failures when the question follows the update immediately, and 8.7% of the same failures when the remaining turns, including a later mention of the old value, run first. Selection must therefore be maintained through the context that follows, not only established at the update (Appendix B.10).

A late change does work. Adding the difference between the probe weights for the current and competing values at the answer position can favor the current value even when the model initially answers incorrectly, and we compare this with an equally large random change (Equation 17). Its advantage grows with strength at the final layer, and the same test near the middle has much smaller effects. At relative strength $\alpha = 0.4$, targeted steering reduces persistence of the original error category by 39.5% more than random steering in Qwen and 69.5% in Llama (Appendix Figure 6). Because it uses the known current value at the final state, this is a diagnostic intervention: it can directly favor the answer without locating the original error. Selection stays open to change at the end of the computation, which is where Section 6 intervenes.

5 A theoretical explanation of old-value selection

Our experiments show that models can return an old value even when the current value remains recoverable from their hidden states. We provide a theoretical explanation using a one-layer Transformer with a simplified copying mechanism: both values remain available, and the probability of copying each value equals the attention weight on its position. This setting lets us examine how selection can fail without information being lost.

Consider a current value v_c and an old value v_o, with attention scores s_c, s_o and distances $d_c < d_o$ from the query. Their selection probabilities $P(\cdot)$ depend on the difference between their attention scores. For a shared content key with rotary position encoding (Su et al., 2024), this relationship becomes

$$\log \frac{P(v_c)}{P(v_o)} = \frac{s_c - s_o}{T} = \frac{2}{T} \sum_b w_b \sin(m\theta_b + \psi_b) \sin\left(\frac{\delta\theta_b}{2}\right), \tag{3}$$

where $T > 0$ is the softmax temperature, $\delta = d_o - d_c$, $m = (d_c + d_o)/2$, and w_b, θ_b, ψ_b denote the amplitude, frequency, and phase of rotary band b.

Equation 3 shows why retaining the current value does not guarantee that it will be selected. When the attention-score difference $s_c - s_o$ is small relative to T, $P(v_c)/P(v_o)$ is close to one, meaning an outdated value is nearly as likely to be selected as the current one.Moreover, because the right-hand side of Equation 3 is not strictly positive, a more recent positional placement alone cannot guarantee a higher attention score (Du et al., 2026). This dynamic provides a clear mathematical explanation for why stale-binding errors occur even when the current information remains perfectly recoverable in our probing experiments. (Detailed derivations are provided in Appendix A.1, and we offer a measured pairwise example in Appendix B.8).

The presence of multiple old values further exacerbates this competition. Given k old values, the ratio of the probability of selecting the current value to that of selecting any old value is $e^{s_c/T} / \sum_{j=1}^{k} e^{s_j/T}$. If we hold existing scores constant, injecting an additional old value strictly decreases this ratio, despite the current value's score remaining entirely unchanged. This accumulation illustrates how successive updates mathematically dilute the likelihood of selecting the current state without ever erasing the underlying information. The central implication is that information retention and attention-based selection are fundamentally distinct requirements: accumulated old values remain formidable competitors for retrieval even when the correct current state is fully available.

6 CONTROLLING SELECTION AT TEST TIME

We test whether redirecting attention from old values to the current value can correct the model's answer without changing its weights (Zhang et al., 2024). This intervention improves current-value retrieval on controlled preference dialogues (Table 2). For comparison, we also append the current value identified by the same parser as an explicit reminder. At inference time, a rule-based parser uses the dialogue's predefined variables, values, and update patterns to identify the current value and its earlier alternatives. Because the parser already identifies the correct value, this experiment tests whether redirecting attention can make the model use it. We adjust selected attention heads at the final prompt position. Let C and O contain the token positions of the queried variable's current and old values, respectively. For each selected head, we add a bias $\beta \geq 0$ to the attention scores at current-value positions and subtract it at old-value positions:

$$s'_j = s_j + \beta\,\mathbf{1}[j \in C] - \beta\,\mathbf{1}[j \in O], \qquad a_j = \frac{e^{s_j}}{\sum_\ell e^{s_\ell}}, \quad a'_j = \frac{e^{s'_j}}{\sum_\ell e^{s'_\ell}}. \tag{4}$$

Here s_j denotes the original attention score, while a_j and a'_j are the attention weights before and after routing, normalized over all prompt positions. The bias β shifts attention toward the current value and away from old values. We consider two forms of routing: a fixed bias calibrated in advance, and an adaptive bias that adjusts to each input to reach a target current-to-old attention ratio, subject to a cap. Heads and routing settings are selected before testing, without using test labels (Appendix E).

Table 2: Accuracy and preservation are percentages; old-error correction is shown as counts.

	Accuracy ↑			Old errors	Preserved
Model	Original	Routing	Reminder	corrected ↑	↑
Adaptive attention bias					
Qwen2.5-3B	16.46	95.21	**99.27**	678/711	98.73
Llama-3.2-3B	27.71	**93.12**	68.85	514/541	100.00
Llama-3.1-8B	41.71	**88.63**	65.38	395/467	100.00
Mistral-7B	5.42	81.35	**98.44**	564/674	98.08
Gemma-2-9B	47.08	**91.88**	82.81	407/455	100.00
Fixed attention bias					
Qwen2.5-7B	37.60	68.85	**88.02**	208/487	100.00
Qwen2.5-14B	40.52	41.67	**98.54**	13/491	98.46

Reminder adds the parsed current value before the query. Old errors corrected shows corrected/initial old-value errors; Preserved shows the percentage of initially correct answers retained.

Adaptive routing improves current-value retrieval while largely preserving answers that were already correct. Across the five adaptive configurations, absolute accuracy gains range from 44.79 to 78.75%, with 98.08 to 100% of initially correct answers preserved (Table 2). These improvements depend on which positions and heads are targeted: all five gains exceed the observed ranges of random-head and random-position controls, while reversing the routing reduces accuracy (Appendix Table 13). Routing also outperforms an explicit current-value reminder in both Llama models and Gemma, although reminders remain stronger in Qwen and Mistral. Together, these results show that directing attention toward the current value can substantially improve answer selection.

7 Related Work

Updating information in context. Memory benchmarks test knowledge and preference updates in conversation (Wu et al., 2025a; Zhao et al., 2025; Jiang et al., 2025) and agent-maintained memory (Cheng et al., 2026; Uddin et al., 2026; Xie et al., 2026; Patel, 2026). Earlier dialogue systems remove invalidated memories (Bae et al., 2022). In-context editing (Zheng et al., 2023) and learned context-dependent unlearning (Takashiro et al., 2025) control factual responses. ICF-Bench evaluates superseded instructions and preferences (Qian et al., 2026).

Interference and knowledge conflicts. PI-LLM establishes declining recall under repeated key–value updates (Wang & Sun, 2025). Our overwrite errors favor recent old assignments, where Chattaraj & Raj (2026) report primacy intrusion under a different protocol. Other work studies cache suppression and quantization (Xie, 2026; Shahrabi-Farahani & Rahmati, 2026). Position effects are studied by Liu et al. (2024); Hsieh et al. (2024b). Knowledge-conflict studies contrast context with parametric memory (Xu et al., 2024; Xie et al., 2024), while context-aware decoding amplifies contextual evidence (Shi et al., 2024).

Binding and selection mechanisms. Entity-tracking tasks (Kim & Schuster, 2023; Li et al., 2025; Wu et al., 2025c) and circuit analyses (Prakash et al., 2024; Feng & Steinhardt, 2024; Gur-Arieh et al., 2026) examine state and binding representations. Tang et al. (2026) find parallel aggregation of state-changing operations at the query position. We instead ask why an updated value remains recoverable when a superseded value is selected. Oh & Demberg (2026) identify retrieval-conditioned rebinding circuits. Retrieval heads identify copying routes (Wu et al., 2025b). We study competition among successive assignments of the same variable. Our Qwen comparison gives distinct, partly overlapping rankings for single-write copying and attention to the latest assignment (Appendix B.5).

Test-time intervention. Activation steering changes outputs through learned directions (Turner et al., 2023; Li et al., 2023). PASTA reweights selected attention heads toward supplied emphasis spans (Zhang et al., 2024). Our routing derives current and superseded spans from dialogue updates, then calibrates heads and intervention strength to redirect selection toward the current value. This tests causal control on direct questions, without changing model weights.

8 Limitations

Our controlled dialogues and constructed operational logs do not estimate failure prevalence in deployed agents. Internal measurements only cover open-source models, with different patterns across comparisons. Probes establish recoverability, while known-answer steering establishes output control. Routing requires internal access, labeled calibration, and a structured parser.

9 Conclusion

Reliable context management requires both retaining updates and using the current state. CICM brings dialogue updates, revised-constraint decisions, and complex operational histories into a common framework for diagnosing update failures. Our open-model experiments show that the current value can remain recoverable even when the answer selects an old one. Probes reveal a selection bottleneck, and component interventions in Qwen and Pythia identify how attention drift toward old values contributes to it. A simple one-layer model explains how old values can collectively receive more

attention than the current value. Training-free attention routing improves direct answers, correcting most old-value errors with input-adjusted interventions across Qwen, Llama, Mistral, and Gemma. The challenge also reaches frontier reasoning models: GPT-5.6 Sol and Claude Opus 4.8 produce incorrect current-state answers on complex histories even when their reasoning completes. Access to the full history and extensive reasoning therefore do not guarantee correct use of an evolving state. Together, our benchmark, mechanism analysis, and interventions make reliable update selection a concrete target for building and evaluating LLM agents.

ACKNOWLEDGEMENT

This work was supported by the U. S. Army Research Laboratory and the U. S. Army Research Office under Grant W911NF2010219, Office of Naval Research under Grant N000142412673, and NSF.

CODE AND DATA AVAILABILITY

The experiment code and CICM benchmark dataset are publicly available at `https://github.com/JamesJunyuGuo/CICM`. The appendices describe the task construction, evaluation protocols, model settings, and statistical analyses.

REFERENCES

John R Anderson. Retrieval of propositional information from long-term memory. *Cognitive Psychology*, 6(4):451–474, 1974.

Sanghwan Bae, Donghyun Kwak, Soyoung Kang, Min Young Lee, Sungdong Kim, Yuin Jeong, Hyeri Kim, Sang-Woo Lee, Woomyoung Park, and Nako Sung. Keep me updated! memory management in long-term conversations. In *Findings of the Association for Computational Linguistics: EMNLP 2022*, pp. 3769–3787, 2022. doi: 10.18653/v1/2022.findings-emnlp.276.

Stella Biderman, Hailey Schoelkopf, Quentin Gregory Anthony, Herbie Bradley, Kyle O'Brien, Eric Hallahan, Mohammad Aflah Khan, Shivanshu Purohit, USVSN Sai Prashanth, Edward Raff, et al. Pythia: A suite for analyzing large language models across training and scaling. *Proceedings of the 40th International Conference on Machine Learning*, 2023.

Sourav Chattaraj and Kanak Raj. LLMs remember first, forget last: Dual-process interference in large language models. *arXiv preprint arXiv:2603.00270*, 2026.

Jiayang Cheng, Dongyu Ru, Lin Qiu, Yiyang Li, Xuezhi Cao, Yangqiu Song, and Xunliang Cai. AMemGym: Interactive memory benchmarking for assistants in long-horizon conversations. In *International Conference on Learning Representations*, 2026. URL `https://openreview.net/forum?id=sfrVLzsmlf`.

Yufeng Du, Phillip Harris, Minyang Tian, Eliu A. Huerta, Srikanth Ronanki, Subendhu Rongali, Aram Galstyan, and Hao Peng. RoPE distinguishes neither positions nor tokens in long contexts, provably. *arXiv preprint arXiv:2605.15514*, 2026.

Jiahai Feng and Jacob Steinhardt. How do language models bind entities in context? In *International Conference on Learning Representations*, 2024. URL `https://openreview.net/forum?id=zb3b6oKO77`.

Gemma Team, Morgane Riviere, et al. Gemma 2: Improving open language models at a practical size. *arXiv preprint arXiv:2408.00118*, 2024. URL `https://arxiv.org/abs/2408.00118`.

Mor Geva, Roei Schuster, Jonathan Berant, and Omer Levy. Transformer feed-forward layers are key-value memories. In *Proceedings of EMNLP*, 2021.

Aaron Grattafiori et al. The Llama 3 herd of models. *arXiv preprint arXiv:2407.21783*, 2024. URL `https://arxiv.org/abs/2407.21783`.

Yoav Gur-Arieh, Mor Geva, and Atticus Geiger. Mixing mechanisms: How language models retrieve bound entities in-context. In *International Conference on Learning Representations*, 2026. URL `https://openreview.net/forum?id=UJ2UUjT2ko`.

John Hewitt and Percy Liang. Designing and interpreting probes with control tasks. In *Proceedings of the 2019 Conference on Empirical Methods in Natural Language Processing and the 9th*

International Joint Conference on Natural Language Processing, pp. 2733–2743, 2019. doi: 10.18653/v1/D19-1275.

Marc W Howard and Michael J Kahana. A distributed representation of temporal context. *Journal of Mathematical Psychology*, 46(3):269–299, 2002.

Cheng-Ping Hsieh, Simeng Sun, Samuel Kriman, Shantanu Acharya, Dima Rekesh, Fei Jia, Yang Zhang, and Boris Ginsburg. RULER: What's the real context size of your long-context language models? *arXiv preprint arXiv:2404.06654*, 2024a.

Cheng-Yu Hsieh, Yung-Sung Chuang, Chun-Liang Li, Zifeng Wang, Long Le, Abhishek Kumar, James Glass, Alexander Ratner, Chen-Yu Lee, Ranjay Krishna, and Tomas Pfister. Found in the middle: Calibrating positional attention bias improves long context utilization. In *Findings of the Association for Computational Linguistics: ACL 2024*, pp. 14982–14995, 2024b. doi: 10.18653/v1/2024.findings-acl.890.

Albert Q. Jiang et al. Mistral 7B. *arXiv preprint arXiv:2310.06825*, 2023. URL https://arxiv.org/abs/2310.06825.

Bowen Jiang, Zhuoqun Hao, Young-Min Cho, Bryan Li, Yuan Yuan, Sihao Chen, Lyle Ungar, Camillo J. Taylor, and Dan Roth. Know me, respond to me: Benchmarking LLMs for dynamic user profiling and personalized responses at scale. In *Conference on Language Modeling*, 2025. URL https://openreview.net/forum?id=6ox8XZGOqP.

Najoung Kim and Sebastian Schuster. Entity tracking in language models. In *Proceedings of the 61st Annual Meeting of the Association for Computational Linguistics*, pp. 3835–3855, 2023.

Yuri Kuratov, Aydar Bulatov, Petr Anokhin, Ivan Rodkin, Dmitry Sorokin, Artyom Sorokin, and Mikhail Burtsev. BABILong: Testing the limits of llms with long context reasoning-in-a-haystack. In *Advances in Neural Information Processing Systems 37 (Datasets and Benchmarks Track)*, 2024.

Belinda Z. Li, Zifan Carl Guo, and Jacob Andreas. (How) do language models track state? In *Proceedings of the 42nd International Conference on Machine Learning*, volume 267, pp. 34429–34452, 2025.

Kenneth Li, Oam Patel, Fernanda Viégas, Hanspeter Pfister, and Martin Wattenberg. Inference-time intervention: Eliciting truthful answers from a language model. *arXiv preprint arXiv:2306.03341*, 2023.

Nelson F. Liu, Kevin Lin, John Hewitt, Ashwin Paranjape, Michele Bevilacqua, Fabio Petroni, and Percy Liang. Lost in the middle: How language models use long contexts. *Transactions of the Association for Computational Linguistics*, 12:157–173, 2024. doi: 10.1162/tacl_a_00638.

John A McGeoch. Forgetting and the law of disuse. *Psychological Review*, 39(4):352–370, 1932.

Kevin Meng, David Bau, Alex Andonian, and Yonatan Belinkov. Locating and editing factual associations in gpt. In *Advances in Neural Information Processing Systems*, 2022.

Kevin Meng, Arnab Sen Sharma, Alex Andonian, Yonatan Belinkov, and David Bau. Mass-editing memory in a transformer. In *International Conference on Learning Representations*, 2023.

Soyoung Oh and Vera Demberg. A retrieval conditioned rebinding circuit for dynamic entity tracking in large language models. *arXiv preprint arXiv:2606.08644*, 2026.

Catherine Olsson, Nelson Elhage, Neel Nanda, Nicholas Joseph, Nova DasSarma, Tom Henighan, Ben Mann, Amanda Askell, Yuntao Bai, Anna Chen, et al. In-context learning and induction heads. In *Transformer Circuits Thread*, 2022.

Vedant Patel. Supersede: Diagnosing and training the memory-update gap in LLM agents. *arXiv preprint arXiv:2606.27472*, 2026.

Nikhil Prakash, Tamar Rott Shaham, Tal Haklay, Yonatan Belinkov, and David Bau. Fine-tuning enhances existing mechanisms: A case study on entity tracking. In *International Conference on Learning Representations*, 2024. URL https://arxiv.org/abs/2402.14811.

Yuli Qian, Zechuan Yang, Wenbiao Ding, Hongzhi Li, and Yutao Xie. Do llms forget what they should? evaluating in-context forgetting in large language models. In *International Conference on Learning Representations*, 2026.

Jeroen GW Raaijmakers and Richard M Shiffrin. Search of associative memory. *Psychological Review*, 88(2):93–134, 1981.

Shayan Shahrabi-Farahani and Dara Rahmati. Compress and forget: bitsandbytes quantization amplifies proactive interference in LLMs. *arXiv preprint arXiv:2608.18578*, 2026.

Weijia Shi, Xiaochuang Han, Mike Lewis, Yulia Tsvetkov, Luke Zettlemoyer, and Scott Wen-tau Yih. Trusting your evidence: Hallucinate less with context-aware decoding. In *Proceedings of the 2024 Conference of the North American Chapter of the Association for Computational Linguistics: Human Language Technologies (Short Papers)*, 2024. URL https://arxiv.org/abs/2305.14739.

Jianlin Su, Murtadha Ahmed, Yu Lu, Shengfeng Pan, Wen Bo, and Yunfeng Liu. RoFormer: Enhanced transformer with rotary position embedding. *Neurocomputing*, 568:127063, 2024. doi: 10.1016/j.neucom.2023.127063.

Shota Takashiro, Takeshi Kojima, Andrew Gambardella, Qi Cao, Yusuke Iwasawa, and Yutaka Matsuo. Answer when needed, forget when not: Language models pretend to forget via in-context knowledge unlearning. In *Findings of the Association for Computational Linguistics: ACL 2025*, 2025. URL https://arxiv.org/abs/2410.00382.

Zilu Tang, Qiao Zhao, Gabriel Franco, Derry Wijaya, Aaron Mueller, Sebastian Schuster, and Najoung Kim. Do language models track entities across state changes? In *Proceedings of the 43rd International Conference on Machine Learning*, 2026. URL https://arxiv.org/abs/2605.30233.

Endel Tulving and Zena Pearlstone. Availability versus accessibility of information in memory for words. *Journal of Verbal Learning and Verbal Behavior*, 5(4):381–391, 1966. doi: 10.1016/S0022-5371(66)80048-8.

Alexander Matt Turner, Lisa Thiergart, David Udell, Gavin Leech, Ulisse Mini, and Monte MacDiarmid. Activation addition: Steering language models without optimization. *arXiv preprint arXiv:2308.10248*, 2023.

Md Nayem Uddin, Kumar Shubham, Eduardo Blanco, Chitta Baral, and Gengyu Wang. From recall to forgetting: Benchmarking long-term memory for personalized agents. *arXiv preprint arXiv:2604.20006*, 2026.

Benton J Underwood. Interference and forgetting. *Psychological Review*, 64(1):49–60, 1957.

Ashish Vaswani, Noam Shazeer, Niki Parmar, Jakob Uszkoreit, Llion Jones, Aidan N. Gomez, Lukasz Kaiser, and Illia Polosukhin. Attention is all you need. In *Advances in Neural Information Processing Systems*, volume 30, 2017.

Chupei Wang and Jiaqiu Vince Sun. Unable to forget: Proactive interference reveals working memory limits in LLMs beyond context length. *arXiv preprint arXiv:2506.08184*, 2025. URL https://arxiv.org/abs/2506.08184.

Olga C Watkins and Michael J Watkins. Buildup of proactive inhibition as a cue-overload effect. *Journal of Experimental Psychology: Human Learning and Memory*, 1(4):442–452, 1975.

Delos D Wickens. Encoding categories of words: An empirical approach to meaning. *Psychological Review*, 77(1):1–15, 1970.

Di Wu, Hongwei Wang, Wenhao Yu, Yuwei Zhang, Kai-Wei Chang, and Dong Yu. LongMemEval: Benchmarking chat assistants on long-term interactive memory. In *International Conference on Learning Representations*, 2025a. URL https://openreview.net/forum?id=pZiyCaVuti.

Wenhao Wu, Yizhong Wang, Guangxuan Xiao, Hao Peng, and Yao Fu. Retrieval head mechanistically explains long-context factuality. In *International Conference on Learning Representations*, 2025b. URL https://arxiv.org/abs/2404.15574.

Yiwei Wu, Atticus Geiger, and Raphaël Millière. How do transformers learn variable binding in symbolic programs? In *Proceedings of the 42nd International Conference on Machine Learning*, volume 267, pp. 67284–67299, 2025c.

Jian Xie, Kai Zhang, Jiangjie Chen, Renze Lou, and Yu Su. Adaptive chameleon or stubborn sloth: Revealing the behavior of large language models in knowledge conflicts. In *International Conference on Learning Representations*, 2024. URL https://arxiv.org/abs/2305.13300.

Wenya Xie, Shengming Zhou, Zelin Li, Pouya Parsa, Shuang Zhou, Xinheng Ding, Chinmay Arvind, Guanchu Wang, Vladimir Braverman, Ali Payani, Yantao Zheng, and Zirui Liu. DynamicMem: A long-horizon memory benchmark in real-world settings. *arXiv preprint arXiv:2606.22877*, 2026.

Ying Xie. Learning to forget: Sleep-inspired memory consolidation for resolving proactive interference in large language models. *arXiv preprint arXiv:2603.14517*, 2026.

Rongwu Xu, Zehan Qi, Zhijiang Guo, Cunxiang Wang, Hongru Wang, Yue Zhang, and Wei Xu. Knowledge conflicts for LLMs: A survey. In *Proceedings of the 2024 Conference on Empirical Methods in Natural Language Processing*, pp. 8541–8565, 2024. doi: 10.18653/v1/2024.emnlp-main.486.

An Yang et al. Qwen2.5 technical report. *arXiv preprint arXiv:2412.15115*, 2024. URL https://arxiv.org/abs/2412.15115.

Michael A Yassa and Craig EL Stark. Pattern separation in the hippocampus. *Trends in Neurosciences*, 34(10):515–525, 2011.

Qingru Zhang, Chandan Singh, Liyuan Liu, Xiaodong Liu, Bin Yu, Jianfeng Gao, and Tuo Zhao. Tell your model where to attend: Post-hoc attention steering for LLMs. In *International Conference on Learning Representations*, 2024. URL https://arxiv.org/abs/2311.02262.

Siyan Zhao, Mingyi Hong, Yang Liu, Devamanyu Hazarika, and Kaixiang Lin. Do LLMs recognize your preferences? evaluating personalized preference following in LLMs. In *International Conference on Learning Representations*, 2025. URL https://openreview.net/forum?id=QWunLKbBGF.

Ce Zheng, Lei Li, Qingxiu Dong, Yuxuan Fan, Zhiyong Wu, Jingjing Xu, and Baobao Chang. Can we edit factual knowledge by in-context learning? In *Proceedings of the 2023 Conference on Empirical Methods in Natural Language Processing*, 2023. URL https://arxiv.org/abs/2305.12740.

APPENDIX GUIDE

The appendices provide derivations, additional evidence, and replication details. For the mechanism results, start with Appendices B.5–B.10.

		Page
A	Theory: assumptions and proofs	13
B	Additional results	18
B.1	Failure examples	18
B.2	Which old value is returned?	19
B.3	Independent community benchmarks	20
B.4	ICF-Bench scoring and answer format	20
B.5	Retained information and attention	21
B.6	Component replacements	21
B.7	Steering at the answer position	21
B.8	Tracing attention in Pythia-160M	23
B.9	Testing a linear account of identity and recency	23
B.10	When old-value answers develop	24
C	Experimental setup and reproducibility	25
D	CICM datasheet	26
E	Test-time attention routing: method, controls, and scope	30
F	Behavioral robustness and task diversity	32
F.3	Task diversity and blinded semantic review	35
F.4	Decisions after scoped updates in dialogues and agent logs	36
F.5	Frontier failures on complex operational histories	39

A THEORY: ASSUMPTIONS AND PROOFS

We give the assumptions and proofs for the one-layer model in Section 5, covering pairwise positional matching and competition among retained assignments.

A.1 ONE-LAYER ATTENTION MODEL

Consider the assignments associated with a single queried variable. Let assignment i at distance d_i from the answer query q receive score $s_i = \langle q, R_{-d_i} k_0 \rangle / \sqrt{d_h}$. We assume these assignments have

the same content key k_0, so their scores differ only through position. Here R_{-d_i} is the RoPE rotation for relative distance d_i, and d_h is the attention-head dimension. Let $T > 0$ be the softmax temperature. The attention weight is $a_i = e^{s_i/T} / \sum_j e^{s_j/T}$. We assume that each assignment carries a distinct answer v_i, that attending to an assignment copies its value faithfully, and that later computation does not change the copied identity. Let Y denote the returned value. Its distribution is then

$$\Pr(Y = v_i) = a_i. \tag{5}$$

Below, $P(v_i)$ abbreviates $\Pr(Y = v_i)$ within this model. Let b be the two-dimensional rotary band, q_b and $k_{0,b}$ be the corresponding query and key blocks, θ_b be the band's angular frequency, ψ_b be the angle between these blocks, and $w_b = \|q_b\|\|k_{0,b}\|/\sqrt{d_h}$ be their content-dependent amplitude. The score of the assignment at distance d from the query is then

$$\varphi(d) = \langle q, R_{-d} k_0 \rangle / \sqrt{d_h} = \sum_b w_b \cos(d\theta_b + \psi_b), \tag{6}$$

Proposition 1 (Pairwise odds identity)**.** *For a current assignment c at distance d_c and an old assignment o at distance $d_o > d_c$, let $\delta = d_o - d_c$ and $m = \frac{1}{2}(d_c + d_o)$. Then*

$$\log \frac{P(v_c)}{P(v_o)} = \frac{s_c - s_o}{T} = \frac{2}{T} \sum_b w_b \sin(m\theta_b + \psi_b) \sin\Big(\tfrac{\delta\theta_b}{2}\Big). \tag{7}$$

Proof. Equation 5 gives $P(v_c)/P(v_o) = a_c/a_o = e^{(s_c - s_o)/T}$ because the softmax normalizer cancels. Applying $\cos A - \cos B = -2 \sin \frac{A+B}{2} \sin \frac{A-B}{2}$ to $\varphi(d_c) - \varphi(d_o)$ gives the final expression. □

Corollary 1 (Pairwise rotary-margin bound)**.** *Define*

$$B(\delta) = \frac{2}{T} \sum_b w_b \left| \sin\left(\frac{\delta\theta_b}{2}\right) \right|. \tag{8}$$

Then we have

$$e^{-B(\delta)} \le \frac{P(v_c)}{P(v_o)} \le e^{B(\delta)}. \tag{9}$$

Consequently, when the band-weighted positional difference $B(\delta)$ is small, the two assignments must have similar selection probabilities.

Proof. Taking absolute values in Equation 7, applying the triangle inequality, and using $|\sin(m\theta_b + \psi_b)| \le 1$ gives $|\log(P(v_c)/P(v_o))| \le B(\delta)$. Exponentiating yields the result. □

Proposition 2 (Single-band translation reversal)**.** *Fix the content and assignment order, and let the pair have separation δ and midpoint m. Translate both assignments by an integer τ. In the single-band model, let w be the band's amplitude, define $A = \frac{2w}{T} \sin(\delta\theta_1/2)$, and write $L(\tau) = A \sin((m + \tau)\theta_1 + \psi_1)$. If $\theta_1 \notin 2\pi\mathbb{Z}$ and L is not identically zero, some integer translations make L positive and others make it negative. Thus the same ordered pair can favor opposite answers at different absolute placements.*

Proof. If $\theta_1/(2\pi)$ is irrational, the integer phase orbit is dense on the circle and visits both open half-circles. If it equals r/ℓ in lowest terms with $\ell \ge 2$, the sum of $L(\tau)$ over one ℓ-point orbit is zero. Because the orbit is not identically zero, it contains both signs. □

For example, take a rotary period of 10, $\psi_1 = 0$, and $w = T = 1$. A current assignment at distance 1 and an old assignment at distance 5 give the current value about 6:1 odds. Translating both assignments by five positions reverses the scores and gives the old value the same advantage, although their order is unchanged. The bound in Corollary 1 is sufficient rather than necessary: rotary bands can also cancel one another and produce near-equal odds when $B(\delta)$ itself is not small. Our empirical QK measurements report the total score margin, not the individual band terms, so we do not interpret them as an estimate of $B(\delta)$.

Proposition 3 (Accumulation of old assignments)**.** *Let $C = \{c\}$ contain the current assignment and let $S_k = \{1, \dots, k\}$ index the old assignments, whose scores are $s_1, \dots, s_k$. Keep these scores and s_c fixed when adding a candidate. For any group G, let $P_k(G)$ denote its total selection probability under the softmax over $C \cup S_k$, and define $F_{S,k} = T \log \sum_{j \le k} e^{s_j/T}$. Adding an old assignment with finite score s_{k+1} gives*

$$\frac{P_{k+1}(C)}{P_{k+1}(S_{k+1})} = \frac{P_k(C)}{P_k(S_k)} \frac{1}{1 + \exp((s_{k+1} - F_{S,k})/T)} < \frac{P_k(C)}{P_k(S_k)}. \tag{10}$$

Proof. Adding $e^{s_{k+1}/T}$ multiplies the old-value partition sum by $1 + e^{(s_{k+1} - F_{S,k})/T} > 1$. The current-to-old odds are therefore multiplied by its reciprocal, which is strictly below one. □

Corollary 2 (Unrelated candidates leave fixed pairwise odds unchanged)**.** *For any additional candidate set D with fixed scores, let P' denote the selection distribution after adding D. Then $P'(v_c)/P'(v_o) = e^{(s_c - s_o)/T} = P(v_c)/P(v_o)$.*

Proof. The additional candidates change the shared softmax normalizer, which cancels in the ratio between the two fixed candidates. □

To describe competition between groups, we also consider a softmax over candidate scores without assuming that they come from a single head. Let C, S, and O denote the current-value, old-value, and other-variable candidate groups. For a group $G \in \{C, S, O\}$ with scores s_i and temperature $T > 0$, write

$$Z_G = \sum_{i \in G} e^{s_i/T}, \qquad F_G = T \log Z_G, \qquad \pi_G = \frac{e^{F_G/T}}{\sum_H e^{F_H/T}}. \tag{11}$$

When restricting the choice to the current- and old-value groups, write $\pi_{C|C \cup S} = Z_C/(Z_C + Z_S)$. These definitions let us compare groups containing different numbers of values.

A.2 RoPE DOES NOT GUARANTEE A GLOBAL RECENCY ORDERING

Proposition 4 (No architecture-guaranteed global recency order under RoPE)**.** *Fix an attention head with rotary position encoding. Let an answer query sit at position n and let a queried variable have assignments at positions $p_1 < \cdots < p_m$ whose keys are identical up to a content perturbation of norm at most η (approximately shared content keys). Then the head's pre-softmax score for assignment j is $\ell_j = g(n - p_j) + O(\eta)$, where $g(d) = \sum_\omega \alpha_\omega \cos(\omega d + \varphi_\omega)$ is a fixed sum of cosines over the head's rotary frequency bands, with $\alpha_\omega, \varphi_\omega$ determined by the query and the shared content key. If g is nonconstant, it is recurrent and cannot be strictly monotone over the unbounded distance domain. Consequently bare RoPE matching does not guarantee that the nearest (most recent) assignment receives the largest score for arbitrary spacings. This global statement does not rule out a particular head being monotone on a finite realized interval.*

Proof. Rotary encoding rotates the query and each key by an angle proportional to position, so the bilinear score between the query at n and a key at p_j depends on positions only through $n - p_j$: writing the shared content key as k_0, $\langle R_n q, R_{p_j} k_0 \rangle = \langle q, R_{-(n-p_j)} k_0 \rangle$, which expands over the rotary frequency bands as $g(n - p_j) = \sum_\omega \alpha_\omega \cos(\omega(n - p_j) + \varphi_\omega)$. A content perturbation of norm $\le \eta$ changes the score by $O(\eta)$, giving $\ell_j = g(n - p_j) + O(\eta)$. If the frequencies are commensurate, nonconstant g is periodic and therefore cannot be strictly monotone over all distances. If they are incommensurate, g is almost periodic: it has arbitrarily large approximate recurrences, which are likewise incompatible with a nonconstant global monotone order. Thus some distance pairs reverse or tie the desired nearest-first ordering whenever their positional-score difference dominates the $O(\eta)$ perturbation. A finite operational interval can still happen to lie inside a monotone segment, which is why the proposition is a lack of an architectural guarantee rather than an impossibility claim for every prompt. □

The proposition concerns a head with approximately shared content keys. A full model can still learn an order-sensitive computation, and rotary encoding alone does not supply the guarantee.

For the full multi-band score, the same calculation yields a weaker but general conclusion: bare rotary matching cannot maintain a uniformly positive recency margin across every placement.

Proposition 5 (No uniform multi-band recency margin)**.** *Fix an ordered current–old pair with separation δ and midpoint m, and translate both assignments by an integer τ. By Proposition 1 the log-odds are $L(\tau) = \frac{2}{T}\sum_b w_b \sin((m+\tau)\theta_b + \psi_b)\sin(\delta\theta_b/2)$, a trigonometric polynomial in τ. If every rotary angle satisfies $0 < \theta_b < 2\pi$ (as for RoPE, whose per-position angles lie in $(0, 1]$) and L is not identically zero, then L has zero Cesàro mean over integer τ. Consequently, there is no $\epsilon > 0$ such that $L(\tau) \geq \epsilon$ for every placement τ.*

Proof. Expand $\sin((m+\tau)\theta_b + \psi_b) = \sin(m\theta_b + \psi_b)\cos(\tau\theta_b) + \cos(m\theta_b + \psi_b)\sin(\tau\theta_b)$. For $0 < \theta_b < 2\pi$ we have $\theta_b \notin 2\pi\mathbb{Z}$, so $\left|\sum_{\tau=0}^{N-1} e^{i\tau\theta_b}\right| = \left|(e^{iN\theta_b} - 1)/(e^{i\theta_b} - 1)\right| \leq 2/|e^{i\theta_b} - 1|$ is bounded in N, giving $\frac{1}{N}\sum_{\tau<N}\cos(\tau\theta_b) \to 0$ and $\frac{1}{N}\sum_{\tau<N}\sin(\tau\theta_b) \to 0$. Summing the finitely many bands, L has zero Cesàro mean. A real sequence with zero Cesàro mean that is not identically zero cannot satisfy $L(\tau) \geq \epsilon > 0$ for all τ. □

Thus the rotary score alone supplies no placement-independent positive margin for the current value. This proposition does not require every multi-band head to reverse its preference on a particular finite context range, but it rules out an architectural guarantee over all placements.

A.3 How score strength and candidate count combine

Proposition 6 (Strength–multiplicity decomposition)**.** *Let $p_i = e^{s_i/T}/Z_G$ be the normalized score within group G, and let $H(p) = -\sum_i p_i \log p_i$ be its entropy. Then*

$$F_G = \sum_{i\in G} p_i s_i + TH(p), \qquad \max_{i\in G} s_i \leq F_G \leq \max_{i\in G} s_i + T\log|G|, \tag{12}$$

Proof. From $\log p_i = s_i/T - F_G/T$, averaging over p_i and rearranging gives the first identity. The lower bound follows because Z_G contains the largest exponential, and the upper bound follows because every term is at most that largest exponential. □

A.4 Selection with bounded score margins

Proposition 3 shows how old assignments accumulate selection mass. Let the current score be $s_c = \mu + \Delta$ and let each of k old-value scores lie in $[\mu - \varepsilon, \mu + \varepsilon]$. The following bounds quantify how group competition grows while the current score remains unchanged.

Proposition 7 (Multiplicity bound)**.** *Conditioned on choosing between the current and old-value groups,*

$$\frac{1}{1 + ke^{-(\Delta-\varepsilon)/T}} \leq \pi_{C|C\cup S} \leq \frac{1}{1 + ke^{-(\Delta+\varepsilon)/T}}. \tag{13}$$

If all old-value scores equal μ ($\varepsilon = 0$), the two bounds coincide.

Proof. Dividing old-value partition mass by current mass gives $Z_S/Z_C = \sum_{j=1}^{k} e^{(s_j - s_c)/T}$. Bounding every summand by the two endpoints yields $ke^{-(\Delta+\varepsilon)/T} \leq Z_S/Z_C \leq ke^{-(\Delta-\varepsilon)/T}$, and substitution into $\pi_{C|C\cup S} = 1/(1 + Z_S/Z_C)$ proves the result. □

Corollary 3 (Retention and selection can separate)**.** *For fixed finite Δ and ε, the current trace and its score may remain unchanged while $\pi_{C|C\cup S} \to 0$ as $k \to \infty$.*

An exact last-write operator could increase Δ with k and escape the fixed-margin regime, and the corollary says only that preserving a representation is insufficient when its selection margin does not grow as quickly as the competing partition mass.

A.5 SELECTING THE LATEST VALUE REQUIRES ORDER INFORMATION

A second special case makes the same point without any score model. If positions are uniformly random and the readout is order-blind — the extreme opposite of a learned recency term — the current value is selected only at chance.

Proposition 8 (Order-invariance excludes latest-binding)**.** *Let the queried variable have $m = k + 1$ assignments whose distinct values are assigned to temporal positions uniformly at random, independent of contents (as in the controlled generators). If the score of each assignment depends only on its content and non-temporal context, then the probability of selecting the latest assignment, conditioned on selecting a value of the queried variable, is exactly $1/m$.*

Proof. Conditioned on contents, an order-blind readout fixes the selection distribution over assignments, while the uniform ordering makes each assignment equally likely to be the latest, independently of that distribution. Hence $\Pr[\text{latest selected}] = \sum_i \Pr[\text{select } i] \cdot \frac{1}{m} = \frac{1}{m}$. □

A.6 COMPETITION BETWEEN OLD VALUES AND OTHER VARIABLES

Write each effective score as a same-variable identity bonus plus remaining contextual evidence. If old values of the queried variable share an identity advantage $b > 0$, let $\widetilde{F}_S$ and $\widetilde{F}_O$ denote the remaining contextual contributions to the old-value and other-variable group scores. Then

$$F_S = b + \widetilde{F}_S, \qquad F_O = \widetilde{F}_O, \qquad \log \frac{\pi_S}{\pi_O} = \frac{b + \widetilde{F}_S - \widetilde{F}_O}{T}, \tag{14}$$

so the boundary between an old-value error and an other-variable error is

$$\widetilde{F}_O - \widetilde{F}_S = b. \tag{15}$$

If moving an old value nearer raises $\widetilde{F}_S$, it strengthens the old-value group without changing the identity bonus b. A nearby value from another variable can instead raise $\widetilde{F}_O$ enough to offset that bonus. This describes the competition in the factorial experiment, but it does not derive a distance-dependent score from RoPE. The candidate counts also matter through Equation 12.

A.7 CONNECTION TO THE MECHANISM EXPERIMENTS

The distinction between information availability and selection is central to our theoretical model. A current value can remain perfectly represented in the hidden state even as competing, outdated values accumulate greater attention weight. Diagnostic probes confirm this availability, while our attention and component-replacement experiments isolate the mechanisms of selection. Similarly, modifying final-layer scores can change the output without repairing upstream computations. While our model formally captures these dynamics, it does not attempt to predict the precise, multi-layer computations of a full network. For example, providing a readout advantage δ to the current value theoretically reduces old-to-current selection odds by a factor of $e^{-\delta/T}$. This dynamic illustrates how answering formats, such as multiple-choice prompts, might shift the error distribution, though it does not prove that multiple choice operates via a single scalar offset. Likewise, the failed linear prediction of identity and recency (Appendix B.9) evaluates a residual-state representation rather than the fixed-head rotary calculation modeled above.

Mechanistic context. Our findings complement existing accounts of Transformer retrieval, including induction heads, key–value memories, and factual-association localization (Olsson et al., 2022; Geva et al., 2021; Meng et al., 2022). We rely on Pythia checkpoints to analyze the emergence of these computations (Biderman et al., 2023), and we utilize shuffled-label controls to validate probe recoverability (Hewitt & Liang, 2019). Furthermore, while methods like ROME and MEMIT permanently edit model weights to update facts (Meng et al., 2022; 2023), our intervention strategy modifies attention directly during inference to observe how dynamic selection shifts the final answer.

A.8 CONNECTIONS TO HUMAN MEMORY RESEARCH

We draw a computational analogy to human memory rather than claiming a shared biological mechanism. Tulving's classical distinction between information availability and accessibility provides

a foundational framework for this analysis (Tulving & Pearlstone, 1966). In proactive-interference experiments, earlier associations directly compete with later ones (Underwood, 1957); similarly, response-competition models distinguish the underlying retention of information from its successful retrieval (McGeoch, 1932). Phenomena such as cue overload, the fan effect, and the SAM sampling model further describe how multiple stored associations compete during retrieval (Watkins & Watkins, 1975; Anderson, 1974; Raaijmakers & Shiffrin, 1981). These cognitive parallels motivate our framing of LLM state-tracking errors as a competition among retained associations.

Additionally, temporal-context models and pattern separation describe mechanisms for distinguishing highly similar experiences (Howard & Kahana, 2002; Yassa & Stark, 2011), while release from proactive interference following a category shift closely parallels our observations regarding variable identity (Wickens, 1970). A critical divergence, however, is that an LLM's context window leaves both earlier and updated statements perfectly visible during processing. Because prompt visibility does not guarantee representation within the model's hidden states, our diagnostic probes and attention interventions remain essential. The cognitive correspondence provides a valuable conceptual lens for formulating hypotheses, but it does not replace rigorous mechanistic testing.

B Additional Results

We first give concrete examples and independent behavioral comparisons, then follow the mechanism from retained information to attention, intervention, and timing. Table 3 separates claims by model and comparison, and the following sections provide their evidence.

Table 3: Mechanistic evidence across models.

Finding	Models	Key evidence
Current values remain readable	Qwen-7B, Llama-8B, Pythia-160M	Held-out probes recover current values on old-value errors, above shuffled-label controls.
Known-answer steering changes output	Qwen-7B, Llama-8B	Final-layer steering compared with equal-norm random directions and middle-layer interventions.
Old-value attention differs by outcome	Qwen-7B, Llama-8B	Failure–correct gap: +19.4 pp in Qwen; +1.2 pp in Llama, whose interval includes zero.
Conflicting updates change internal matching	Five models	Updates versus matched no-update prompts; the shift also occurs on correct answers.
Specific components affect selection	Qwen-7B, Pythia-160M	Qwen: old-assignment key replacement. Pythia: held-out head removal and key-input replacement.

Pythia's probe is evaluated separately. Known-answer steering is a diagnostic intervention. Attention gaps are adjusted for prompt length and reported in percentage points (pp). Appendix B.10 details the matched-context comparisons. Untested comparisons are not null results.

B.1 Examples of old-value and other-variable errors

The following excerpts retain the original prompt and response wording, and only the bracketed dialogue spans are omitted. They show the old-value and other-variable outcomes summarized in the main text.

A clarified CICM dialogue and its answer. Selected user turns from a 44-message dialogue; intervening messages are omitted. Distances count messages before the question.

User. I think **visual** works best for me overall. old value · 40 before

User. I actually prefer **reading** when I'm trying to understand something new. current value · 36 before

User. I'd like to update my preference to **electronic**. another variable (music) · 10 before

User. For the record, **visual** was an earlier choice for my learning style, and is no longer current. explicitly obsolete · 2 before

User. For my learning style specifically, what value did I set in my most recent explicit update? Later mentions of earlier choices are not updates. Ignore preferences for other slots. Reply with only the value.

Qwen2.5-7B. visual

Expected: reading **GPT-4o on the same prompt:** Reading. This uses both clarification treatments in Appendix F.1; the original source dialogue has one earlier value of the queried variable.

An anchored query returns a value of another variable

System. You are a helpful assistant in an ongoing preference-planning conversation.

User. Please set my favorite genre as folk.

Assistant. Your choice has been saved.

User. Switch my music category to classical.

Assistant. The update is complete.

[22 turns omitted]

User. Can you set my meal style to pescatarian?

Assistant. Absolutely, I've saved your updated selection.

[2 turns omitted]

User. Look back at the updates for my music genre. What is the current value for that exact slot, not any other preference? Reply with only the value.

Assistant. pescatarian

Expected: classical **Model:** pescatarian

Gray, blue, and sand boxes denote system, user, and assistant turns. Violet text marks the produced old or otherwise incorrect value; green text marks the current target.

B.2 Which old value is returned?

We re-score saved responses by the queried variable's assignment order. Rank 1 is the most recent old assignment and rank k is the first write, and the current assignment is excluded. Parsing every synthetic prompt verifies that `stale_values` follow chronological write order. For CICM, message positions and value spans verify the recorded binding order and that each near-old re-mention repeats the most recent old value.

Table 4: Most-recent-old responses, conditional on an old-value error. Qwen-7B pools 20/40/80-line prompts; the larger models use 320 lines. The first write is never returned in these cells.

Model	k	Most recent old / old errors	Uniform reference
Qwen2.5-7B	2	54/54 (100.0%)	50.0%
Qwen2.5-7B	4	92/113 (81.4%)	25.0%
Qwen2.5-7B	8	72/164 (43.9%)	12.5%
Qwen2.5-72B	64	7/11 (63.6%)	1.6%
Llama-3.1-70B	64	8/16 (50.0%)	1.6%
GPT-4o	64	3/7 (42.9%)	1.6%

These are descriptive, post-hoc shares conditional on an old-value error, and $1/k$ is a uniform-choice reference, not an estimated error model. The larger-model cells have few old-value errors. In the original CICM core, for $k = 2, 3, 4, 6$, the re-mentioned value accounts for 94.5–100% of old-value responses across both models. Without it, rank 1 accounts for 66.7–100% in Qwen and 44.2–61.1% in Llama. This separates recency among assignments from the additional effect of re-mentioning one of them.

B.3 INDEPENDENT COMMUNITY BENCHMARKS

We test whether related binding errors occur in datasets that were not constructed for this project. BABILong and Entity Tracking permit a strict old-state label: a wrong prediction is an old-value error only when it exactly equals an earlier state of the queried entity or box (Kuratov et al., 2024; Kim & Schuster, 2023). Under audited scoring, 1.4% of BABILong baseline errors and 25.9% of Entity Tracking errors meet this strict definition. Most BABILong errors therefore do not fit this definition.

RULER variable tracking measures a different failure. Its output often includes values from the wrong reference chain: 99.5% of strict baseline failures have a cross-chain inclusion, while mean per-variable recall is 36.7% (Hsieh et al., 2024a). We do not relabel these as old-value errors because the task tests chain tracing rather than an old state. These benchmarks extend the evaluation beyond our templates, but test different kinds of information tracking.

The baseline evaluations contain 1,200 BABILong, 600 Entity Tracking, and 400 RULER-VT examples. Their respective accuracy, set accuracy, and per-variable recall are 46.2%, 47.3%, and 36.7%.

B.4 ICF-BENCH: SCORING AND ANSWER FORMAT

ICF-Bench uses scenario-specific scoring rather than the controlled taxonomy in Section 3. Dynamic Preference multiple choice is scored programmatically. The earlier deterministic matchers were checked on 150 released human-alignment items per scenario, with agreement of 93.0% for Dynamic Preference and 92.3% for Instructional Forgetting.

Free-form preference labels and uncertainty. Exact and unambiguous Dynamic Preference responses are classified deterministically, and GPT-4o assigns the remaining 577 of 783 responses to current, old, or other using the known preferences. The resulting old-value share is 197/240 = 82.1% of errors: deterministic labels contribute 111 old answers, and judged labels contribute 86 old and 43 other answers. On the 40-example human calibration set, hybrid labels agree on 36 examples, and only 13 examples are human-labeled failures. All four disagreements change current versus other, so uncertainty affects the failure denominator too.

The 95% bootstrap interval 77.1–87.1% conditions on assigned labels and does not include annotation error. As a sensitivity analysis, holding deterministic labels fixed but allowing up to 10 of the 577 judge labels to change arbitrarily gives an old-value share of 77.9–86.2%, and allowing 20 gives 73.8–90.4%. These are assumption-indexed ranges, not confidence intervals or estimated annotation error rates. The small calibration set does not establish a population error rate or a statistical upper bound.

Free-form and multiple-choice accuracies are 69.3% and 70.9%, respectively, but the labeled old-value shares differ: 82.1% versus 29.4%. Table 5 reports the point estimates, and the label-conditional qualification applies to all free-form estimates, including Figure 2c.

Table 5: Accuracy and old-value errors on ICF-Bench under different answer formats. Both result columns are percentages; the last is conditional on an error.

Model / task	Answer format	n	Accuracy	Old / errors
ICF-Bench, Qwen2.5-7B				
Dynamic Preference	Free-form	783	69.3	82.1
Dynamic Preference	Multiple choice	783	70.9	29.4

Dynamic Preference free-form labels partly use a model judge; their sampling intervals condition on these labels. Instructional Forgetting's separate content-reuse audit appears in Appendix B.4.

Instructional Forgetting. A separate content-reuse audit flags 918/933 saved responses (98.4%). Disclosure takes precedence over a subsequent promise to withhold the content. This is a programmatic count, not validated semantic accuracy: a targeted source audit finds both missed content matches and ambiguous remaining labels. We therefore exclude it from the cross-task accuracy comparison.

B.5 Retained information and attention on CICM failures

Both models retain information about the current value on failed trials, but only Qwen shows a clear shift toward old assignments in this attention measure. Figure 5b compares Qwen's 471 correct and 589 old-value answers. Table 6 separates the probe's probability for the correct value from the attention allocated to old mentions, and these are different measurements, not two estimates of accuracy.

Table 6: Current-value information remains readable on CICM failures. Probe entries are mean probabilities assigned to the current value, expressed as percentages, not classification accuracy.

		Probe score (%)		Failure − correct (pp)	
Model	n	Old-value errors	Other-variable errors	Probe	Attention
Qwen2.5-7B	1200	84.8	86.5	-7.5	$+19.4$
Llama-3.1-8B	1200	82.2	86.3	-7.3	$+1.2$

The two error columns distinguish answers using an old value of the queried variable from answers using another variable's value. The difference columns compare old-value errors with correct answers, adjusting for prompt length; attention is the share on old assignments. Label-randomized probe scores range from 3.2% to 6.4%. Here n is the full dialogue set, not each error subset.

After accounting for prompt length, the old-attention difference between failed and correct trials has a 95% interval of 17.9 to 21.0 % in Qwen and -0.5% to 2.8% in Llama. The latter does not distinguish a shift from zero. High probe scores on both models' failures therefore support retained information, not a shared attention-level explanation. Appendix C.1 defines the probe and the length adjustment.

Single-write retrieval and update selection. We compare the update-task head ranking with a simplified retrieval-head detector based on Wu et al. (2025b). On 200 fresh single-write prompts (100 each at 40 and 80 lines, seed 30), Qwen2.5-7B-Instruct achieves 97.5% accuracy and produces 771 copied answer tokens. Among these copied tokens, a head's retrieval score is the fraction for which its maximum-attention position lies in the target value span and contains the generated token. The update-task score p_{last} is the attention mass on the latest assignment divided by mass on all assignments of that variable, averaged over correctly answered overwrite prompts. Only two of the top eight p_{last} heads appear among the top sixteen retrieval heads (L22H1 and L23H11, zero-based indices), and the all-head Spearman correlation is -0.021. Thus single-write copying and selection among competing writes produce different head rankings, with some shared components.

B.6 Which computations change the answer?

Replacing late hidden states or the keys of old assignments recovers much more of Qwen's answer-score gap than replacing early or middle hidden states. For each failed prompt, we construct a successful counterpart with the same candidate values and positions, renaming earlier assignments to remove competition for the queried variable. We then replace one component at a time with its counterpart from the successful run (Table 7). The final attention row is an observed difference, not an intervention.

B.7 Steering at the answer position

The targeted change becomes more effective as its strength increases at the final layer, unlike an equally large change in a random direction (Figure 6). At strength 0.4, its advantage over random is 39.5% for Qwen and 69.5 for Llama. Middle-layer effects are much smaller (Table 8).

The outcome is persistence of each item's original error category, not old-value rate alone: the selected cohorts contain 589 old-value and 76 other-variable errors for Qwen, and 634 and 88 for Llama. Local no-change decoding reproduces the original category on 643/665 and 622/722 items. These rates differ from 100% because selection used earlier API labels, and the zero-strength hook exactly reproduces the local no-hook response on every item. At strength 0.4, targeted-minus-random current-answer gains are 35.5% in Qwen and 70.5% in Llama, so reduced category persistence is accompanied by more correct answers.

Table 7: Component replacements and attention differences in Qwen2.5-7B. Recovery is the percentage of the successful–failed answer-score gap restored.

Component	Measurement	Mean	Median	n
Answer-score-gap recovery (%)				
Residual stream	Early / middle layers	−0.5	0.0	600
	Late layers	78.1	93.9	360
Key	Old assignments	49.2	44.8	120
	All assignments	11.1	10.7	120
	Current assignment	−21.3	−19.5	120
Query	Final	11.2	10.9	120
Head / MLP	Head-output proxy	36.0	34.8	120
	Late MLP output	13.2	10.5	960
Successful − failed attention (percentage points)				
Selected heads	Attention to current value	13.0	13.1	120

For recovery, n counts replacements across 120 matched pairs, not independent prompts; negative values move the answer further toward the old value. The head-output row uses a projection-level proxy. The final row is an observed attention difference, not a replacement experiment.

These interventions use the known current value to choose the direction. They test whether the answer can be changed, rather than providing a general correction method that can infer the right value unaided. Equation 17 defines the intervention and its strength.

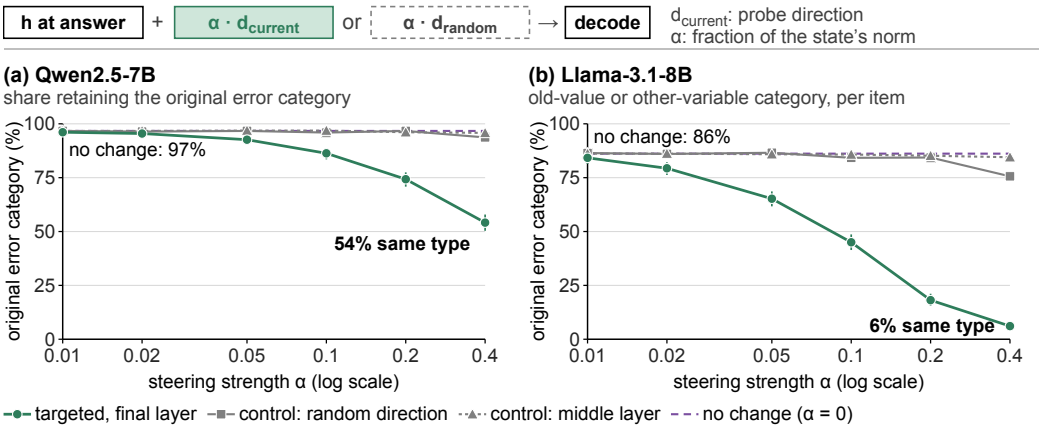

Figure 6: Steering with the known current value. The outcome is persistence of each prompt's original error category (old value or other-variable value), not old-value rate alone. The no-change rates are 643/665 (97%) for Qwen and 622/722 (86%) for Llama: local re-decoding need not reproduce the earlier API label, but $\alpha = 0$ exactly matches the local no-hook response. Bars: 95% Wilson intervals. Paired comparisons and cohort definitions in Appendix B.7.

Table 8: Reduction in original-error-category persistence from targeted steering beyond an equally large random change. Entries are percentage-point differences at strength $\alpha = 0.4$.

Model	Failed trials	Middle layer	Final layer
Qwen2.5-7B	665	−1.1	39.5
Llama-3.1-8B	722	1.8	69.5

Positive values mean less persistence of the originally observed error category (old value or other-variable value) under targeted steering. Both interventions are evaluated on the same failed trials. The full dose response appears in Figure 6.

B.8 TRACING ATTENTION AND ITS INPUTS IN PYTHIA-160M

A small set of attention heads accounts for most of the measured recovery, but removing the heads that favor the current value has no specific effect beyond random removal. We test Pythia-160M with three few-shot templates, three seeds, and single-token values. At four overwrites, the behavioral sample contains 648 prompts: 466 correct, 142 old-value, and 40 other responses (71.9% accuracy, with old values accounting for 78.0% of errors). The mechanism subset balances 142 correct and 142 old-value responses, and 96 matched successful–failed pairs pass the component-replacement checks. After adjustment for prompt length, the probe assigns the current value 32.0 percentage points less probability on failed than correct trials.

We rank heads on 43 discovery pairs and evaluate replacements on 53 held-out pairs. Replacing twelve of the 144 heads recovers 0.81 of the answer-score change obtained by replacing all heads. The largest individual contributions are 0.36 for L8H10, 0.19 for L8H2, and 0.10 for L10H7. Recovery levels off near 0.86 as more ranked heads are added. Table 9 separates where these heads attend (QK) from what their value vectors transmit (OV): on errors, the QK score difference turns against the current value, while its OV contribution changes little.

Table 9: Two Pythia-160M heads attend less to the current value on old-value errors, while their value-transmission margins remain positive. Each column averages 48 examples.

Head	Measurement	Correct answer	Old-value answer
L8H10	Current-value QK margin	1.70	−0.26
	Attention to current value	0.75	0.40
	Current-value OV margin	0.67	0.64
L8H2	Current-value QK margin	1.86	−6.31
	Attention to current value	0.57	0.08
	Current-value OV margin	0.20	0.18

The QK margin is the current assignment's attention score minus the strongest old assignment's score. The OV margin measures how strongly the current assignment's value vector favors its own token over the strongest alternative, before attention weighting. Attention entries are weights, not margins. L8H10: layer 8, head 10.

An empirical example of comparable attention odds. In Pythia-160M head L8H10, the mean current-minus-strongest-old query–key margin over 48 old-value failures is -0.26. With the standard attention softmax ($T = 1$), this gives geometric-mean pairwise attention odds of about $0.77{:}1$, only a $1.30{:}1$ advantage for the old assignment. Mean attention is 0.40 for the current assignment and 0.60 for old assignments combined (Table 9). Thus comparable attention odds occur in a measured head, not only in the theoretical example. They are also answer odds under the faithful-copy assumption of Section 5, but this assumption need not hold for the full model. These measurements do not isolate the contribution of RoPE.

Removing heads selected to promote old values corrects 38.4% of held-out errors, compared with 8.7% for layer-matched random sets (Table 10). The targeted bootstrap interval is 27.4–49.3%, and the empirical 95% range across 64 random sets is 0.8–29.9%. An earlier estimate used the same examples for selection and evaluation and was higher by 6.4 points, and we use the held-out estimate here. Removing heads selected to promote the current value is no more effective than random removal at inducing old-value errors. Replacing queries and keys separately implicates L8H2's keys: the query-minus-key recovery interval is $[-1.62, -1.00]$, whereas L8H10's interval, $[-2.40, 4.53]$, does not resolve the two contributions. Replacing the upstream inputs to L8H2's key recovers 0.86 of the QK score gap and 0.75 of the final answer-score gap, and the corresponding random-set upper 95% bounds are 0.16 and 0.17. The upstream components, ranked on discovery data, are L7H7, L6H2, L7H4, L5H11, L4H11, L5H10, L3H0, L6H6, L5H8, L3-MLP, L3H4, and L4H1. These results identify inputs that affect key matching, but the tests do not establish that these components encode assignment order.

B.9 TESTING A LINEAR ACCOUNT OF IDENTITY AND RECENCY

We fit linear identity and recency scores on training dialogues and evaluate candidate selection on held-out dialogues and six held-out factorial conditions. Combining the scores predicts Qwen's

Table 10: Held-out interventions in Pythia-160M. Random controls use equally sized sets matched by layer; entries are mean fractions or normalized recovery.

Intervention	Measured effect	Targeted	Random
Remove heads favoring old values	Fraction of errors corrected	0.38	0.09
Remove heads favoring the current value	Fraction switching to an old value	0.04	0.03
Replace inputs to L8H2's key	QK score-gap recovery	0.86	0.04
	Answer-score-gap recovery	0.75	0.06

Head removal is tested on 73 old-value errors or 81 correct answers, respectively; key-input replacement uses 53 held-out pairs. Component sets are selected on separate discovery examples. Recovery is normalized by the difference between successful and failed runs: 0 means no recovery and 1 means full recovery. Random entries are means, not upper bounds.

answer on 43.0% of 1,136 examples and Llama's on 39.6% of 1,180, compared with 79.2% and 67.4% for identity alone (randomized-label range: 12.5–16.6%). The combined rule predicts no other-variable errors, although both models make them, and the mean absolute errors for these rates are 24.2 and 17.4 percentage points. Thus the measured scores do not provide an adequate linear account of the response distribution.

B.10 When old-value answers develop

Old-value answers can develop after the update, as the model processes later text. To measure this timing, we truncate each conversation after the first assignment, the update, unrelated text, and the final question. We append the same diagnostic question to each truncated conversation and run a separate forward pass. This avoids treating an earlier token's stored key and value as if they changed when later text was added. Each conversation also has a comparison prompt with the same token count but no conflicting update.

Pythia-160M produces 129 old-value answers and 15 correct answers in 144 trials, yielding 121 valid failure–control pairs. The other models have too few errors for reliable failure-conditioned analysis: Pythia-1.4B, Qwen-1.5B, Qwen-7B, and Llama-8B produce 1/144, 8/144, 1/72, and 2/72 old-value answers, respectively. Gemma-2B produces 14 old-value and 62 other answers in 144 trials, and its no-update control is unreliable.

Among 121 matched Pythia-160M failures, 39 already favor the old value immediately after the update, while the other 82 favor it only after later text. The probe's mean probability for the current value falls from 0.81 after the update to 0.35 at the final question, but remains above the randomized-label ceiling near 0.22. Thus the current value becomes harder to recover without disappearing altogether. Restoring the correct key match prevents 93% of errors when the question immediately follows the update, but only 9% after the remaining conversation (Figure 7). The four no-change checks correct no errors.

Across the five models with reliable controls, the conflicting update shifts attention and key matching toward the old value, even when the final answer remains correct (Figure 5d). Every stage after the update shows this shift relative to a prompt with the same token count but no conflict (all 20 comparisons have the same sign). This shared shift does not by itself explain the larger models' rare errors.

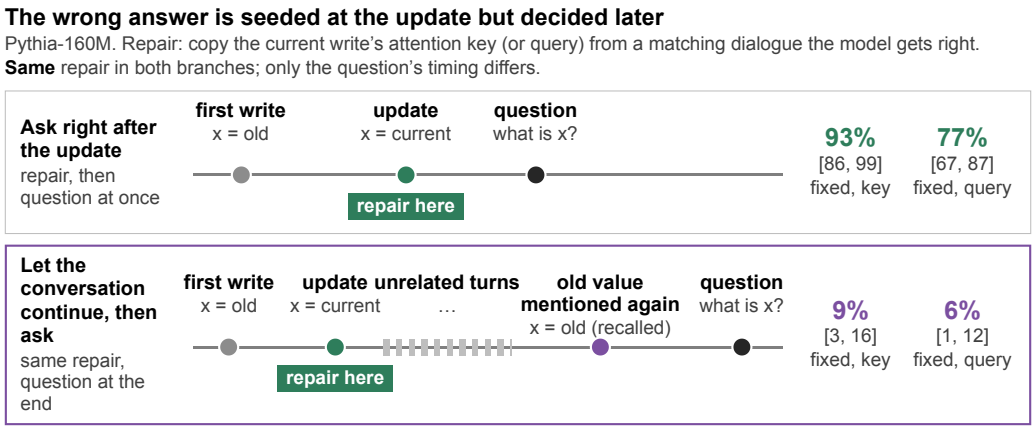

Figure 7: The wrong answer is seeded at the update but decided later. The same repair fixes 93% (key) and 77% (query) of test failures when the question follows the update immediately, but only 9% and 6% once the remaining turns, including a later mention of the old value, precede it. Identity patches fix none.

C Experimental Setup and Reproducibility

Unless stated otherwise, generation is greedy (temperature zero). We score saved responses and estimate uncertainty by resampling examples, not by sampling repeated model answers.

The open-model families include Qwen2.5 (Yang et al., 2024), Llama 3 (Grattafiori et al., 2024), Mistral (Jiang et al., 2023), and Gemma 2 (Gemma Team et al., 2024). Exact variants accompany each experiment.

C.1 Probe and intervention definitions

Linear probe. Let v_i^* be the current value in dialogue i and $r_i^{(\ell)}$ its answer-position hidden state at layer ℓ. The multinomial linear probe is

$$q_\phi(v \mid h_i) = \mathrm{softmax}(Wh_i + b)_v\,, \qquad h_i = z\Big(r_i^{(\ell)}\Big)\,, \tag{16}$$

where $\phi = (W, b)$ are learned parameters and z standardizes each feature using training-fold statistics only. The main analysis uses the final-layer state and predicts one of 21 recurring values. Five-fold cross-validation groups examples by dialogue, so all reported predictions come from a probe that did not train on that dialogue. We compare it with the same procedure after randomly reassigning value labels, preserving the inputs and label frequencies but removing their systematic relationship (Hewitt & Liang, 2019). The final states are taken from Qwen layer 28 and Llama layer 32. We use 2,000 randomized-label repetitions and 2,000 bootstrap replicates (seed 20260721), including randomized-label checks of the length-adjusted comparison.

Across 1,200 dialogues, held-out classification accuracy is 91.2% for Qwen2.5-7B and 89.7% for Llama-3.1-8B. This differs from the mean probability assigned to the current value on old-value failures (84.8% and 82.2%) and other-variable failures (86.5% and 86.3%). The randomized-label range is 3.2–6.4%. To compare successful and failed trials, we fit the relationship between probe score and prompt length once across both groups: $q_\phi(v_i^* \mid h_i) = a + b \log L_i + \epsilon_i$, where L_i is the prompt token count. Group differences in the residuals ϵ_i are -7.5 and -7.3 percentage points for old-value failures relative to correct responses. The probe establishes linear recoverability, but it does not establish that the unmodified model uses this information. The probe learns a readout distinct from the native language-model output head. Recovering the last-update feature is therefore compatible with the model producing an old value, and the measurement concerns recoverable task information, not a belief state.

Normalized intervention. For a probe direction d and residual vector h, the intervention is

$$h' = h + \alpha \|h\|_2 \frac{d}{\|d\|_2}, \tag{17}$$

so α specifies the added vector's norm relative to the original state. We compare each targeted direction with a random direction of identical norm and check that $\alpha = 0$ reproduces the unmodified response.

Synthetic controls. Figure 2a pools 100 examples at each of 20, 40, and 80 lines (300 per column). Length amplifies the update effect: accuracy is 91/85/70% at $k = 2$ and 51/45/38% at $k = 8$, respectively. Panel b uses 20-line contexts with $n = 150$ at $k = 2, 4, 8$ and $n = 100$ at $k = 12, 16$, and 320-line conditions use $n = 50$. Every model's matched no-overwrite control scores 100%. Panels a–b show 95% Wilson intervals, while panel c uses label-conditional bootstrap intervals (Appendix B.4). These sweeps use greedy decoding, a 16-token cap, and data seeds 0 and 40 for the standard and 320-line conditions, respectively. The parallel-variable task interleaves or groups assignments to independent named variables and asks for every variable's latest value. Values are distinct within a prompt, allowing old values of the correct variable to be separated from cross-variable copies. In the component-replacement control, only earlier assignments' variable names change to fresh names of the same character length, while values, line positions, the final target assignment, and the query remain fixed. This removes earlier writes to the queried variable without removing their text (Appendix B.6).

C.2 Evaluation and analysis settings

Behavioral evaluation. The CICM preference core uses the same 1,200 dialogues for Qwen2.5-7B-Instruct and Llama-3.1-8B-Instruct through OpenRouter (16-token cap, data seed 20260723): 200 dialogues per distance condition and 40 per count–distance combination. For ICF-Bench, Qwen evaluates 783 Dynamic Preference examples per answer format with a 160-token response cap, while GPT-4o adjudicates only unresolved labels with a 120-token cap. The 933-example Instructional Forgetting content-reuse audit uses a local 192-token cap. The extended CICM tasks and their scoring contracts are described in Appendix D, and model-specific API settings accompany their results in Appendix F.

Component replacement and steering. Component replacement uses 120 matched successful–failed pairs selected from 301 candidates (pair seed 50), with Qwen2.5-7B in fp32 eager mode and batch size one. We measure recovery of the current-minus-old answer-score gap and verify a no-change control. Residual steering tests the same 665 Qwen and 722 Llama failure items at each relative strength $\alpha \in \{.01, .02, .05, .1, .2, .4\}$, at Qwen layers 13/27 and Llama layers 15/31 (seed 20260722). Paired bootstrap comparisons contrast targeted and equal-norm random changes, and $\alpha = 0$ must reproduce the original response. These intervention counts refer to failed trials, not new independent dialogues.

Behavioral evaluations use API inference. Hidden-state, attention, component replacement, and steering experiments run on an NVIDIA H100 with PyTorch 2.6 and Transformers 4.51. Appendix E gives the separate settings for the cross-model attention-routing experiments. Appendix F gives the paired API checks of update semantics, output budget, and concise reasoning.

D CICM Datasheet

Controlled In-Context Memory (CICM) is a diagnostic evaluation suite for updating and using information in context. Its mechanism core uses preference content from PrefEval (Zhao et al., 2025), and its extensions add multi-field dialogues, decisions under revised constraints, and dependent operational-state updates. Decision catalogues, transition ledgers, and agent logs are constructed for these extensions. Explicit update rules and programmatic answers connect the components, while each retains its own task and scoring contract.

D.1 BENCHMARK COMPONENTS

Table 11 distinguishes the original mechanism core from the broader behavioral evaluations. Sample sizes count the units shown, and multiple prompt conditions from one scenario are paired observations. The suite is not summarized by pooling these different tasks into a single accuracy. All components are constructed diagnostics rather than sampled deployment traces.

Table 11: CICM components and their roles. Sizes refer to the reported cohorts, and separate development checks and repeated conditions are not additional cases.

Component	Cohort	Task	Role
Preference core	1,200 dialogues	Repeated preference updates with competing mentions	Retention, selection and causal interventions
Dialogue diversity	180 pilot ledgers	Scalar, partial-record and full-record updates in six domains	Language and task variation
Constraint decisions	24 scenarios	Booking and scheduling under revised constraints	Use of updated state in decisions
Operational histories	40 + 40 scenarios	Dependent handoffs across 16 slots in warehouse and build-release logs, and a deferred-log tier resolves pending handoffs at later lines	Frontier reasoning under complex and dependency-aware state updates

Mechanism and attention-routing analyses use the preference core, and the other components test behavior. The following sections specify their construction and scoring. Model outcomes and inference settings appear with their experiments in Appendix F.

D.2 PREFERENCE CORE

Vocabulary and design. The preference-core behavioral and mechanism experiments use 1,200 dialogues. The vocabulary contains 21 values across three variables. Music genre covers jazz, rock, classical, electronic, folk, hiphop and blues. Meal style covers vegan, vegetarian, keto, mediterranean, paleo, pescatarian and gluten free. Learning style covers visual, hands on, lecture, reading, discussion, self paced and tutoring.

Each variable contributes 400 examples. Every variable–current-value pair occurs 57 or 58 times, so probes can learn each value from multiple dialogues. The current value of the queried variable is always far from the final question.

We vary both the number of old assignments and their distance from the query. Each dialogue has an overwrite count $k \in \{1, 2, 3, 4, 6\}$ and one of six distance conditions formed by $\{$near, far$\}$ distance for the nearest old value of the queried variable crossed with $\{$far, middle, two turns$\}$ distance for the nearest value of another variable. The design contains 240 dialogues per overwrite count, 200 per distance condition, and 40 per combination. The accuracy decline from 47.1% to 31.7% as old assignments increase from one to six averages over distance conditions, and the factorial comparison averages over overwrite counts.

Each dialogue also includes three post-update assignments to other variables, six standard filler turns, and four additional interference turns. The final query names the queried variable and explicitly excludes other preferences. These choices hold variable identity fixed while crossing old-value reminder conditions with other-variable positions.

Construction and checks. GPT-4.1 generates reusable dialogue template packs for openings, update acknowledgments, and coherent filler turns. The model does not choose any experimental value, answer, position, distance cell, or label. The program injects the exact controlled values into one-placeholder update templates, constructs the ordering, and appends the anchored query. Thus the generated wording varies while values and positions remain controlled. Template validation rejects a pack if an update does not contain exactly one value placeholder, an assistant acknowledgment

repeats the placeholder, or an opening, filler, or query contains any controlled value. Validation of each dialogue then requires all of the following. The current value is absent from the old-value set. The number of old assignments equals k. The query names the queried variable. Exactly one target mention is marked current. Every recorded role, character span, and value mention matches the rendered message. Every distractor update belongs to a different variable. Generation aborts on any violation, and all 1,200 dialogues pass these checks.

Update and mention semantics. The target label is the last explicit assignment in the generator's update sequence. Near-old dialogues add a later user turn saying "I am still thinking about [old value] when I compare options for my [slot]." Its label is a reminder, whereas far-old dialogues omit that turn. All 600 near-old examples contain it and none of the 600 far-old examples do. Thus this contrast changes mention count and wording as well as the nearest old-value position. Naming the target variable in the query resolves which preference is queried, but does not instruct the model that this later mention cannot be an update. The structural checks above establish consistency with the generator's labels, not agreement with an independent semantic judgment.

At $k = 1$, the pooled 47.1% accuracy is 113/240: 25/120 in near-old conditions and 88/120 in far-old conditions. Across all update counts, the 600 far-old examples contain 396 current and 82 old-value answers despite having no added old-value reminder. These subsets describe the existing factorial, but they are not a paired wording ablation or a human/strong-model ceiling. The reported mechanism and routing experiments use this original factorial and its explicit-assignment labels. The paired wording, query, and matched-placement follow-ups, including GPT-4o, appear in Appendix F.1. A separate extension adds three domains, partial- and full-record updates, and dialogue surfaces from three generation models (Appendix F.3), but it does not replace the original mechanism dataset.

Response scoring. Responses are lowercased, punctuation is replaced by spaces, and whitespace is collapsed. Whole normalized value phrases are then matched against the current value, the old-value set, unused values of the queried variable, and values belonging to other variables, in that order. The output label is therefore determined by fixed vocabulary membership, without an LLM judge. Unit tests cover current, old-value, unused same-variable, other-variable, and unmatched responses. Re-scoring the saved Qwen2.5-7B API responses yields 471 current, 589 old-value, 76 other-variable, and 64 other outputs, with no API call-error rows.

The core behavioral run uses Qwen2.5-7B-Instruct with free-form answers capped at 16 tokens. The same stored dialogues and programmatic labels define the Qwen and Llama mechanism subsets, and hidden-state probes never replace the behavioral matcher.

D.3 Multi-field dialogue updates

The diversity cohort contains 180 pilot ledgers crossing six domains, three update structures, and two old-value loads ($k = 1, 4$), with five ledgers per cell. Meeting-room assignment, delivery pickup point, and document output format extend the core's three preference domains. The tasks distinguish replacement of a single value, patches to a three-field record that preserve unmentioned fields, and full-record replacement. Executing the ledger gives the current target value, its previous values, and competing values of other fields.

Each ledger has four paired prompts: template or model-generated language, crossed with near or far placement of the same explicitly obsolete mention. Each contains 24 user–assistant pairs. The current assignment is 30 messages before the question, and the obsolete mention is four or 24 messages away. Swapping its complete pair with value-free filler preserves all other assignments and mention counts. The question explicitly excludes historical mentions from the update sequence.

GPT-5, Claude Sonnet 5, and Gemini 3.8 Flash each render 60 ledgers, plus six pipeline-check ledgers. GPT-5 and Gemini use medium reasoning. Gemini uses temperature 0.7, and Sonnet uses disabled thinking. Generation starts with an 8,192-token cap, extended to 16,384 for truncated GPT-5 outputs. Schema and value-span checks and independent agent review validate the surfaces. At most two automated repairs are allowed, and three surfaces additionally receive logged agent-authored clarifications. All 720 pilot prompts and the scorer are frozen before evaluator answers, and initial outputs and repairs are retained.

A subsequent blinded semantic audit samples 50 distinct ledgers using metadata alone, covering every domain–task–load cell and balancing near/far placement and update load. GPT-6 Astra receives the dialogue but not program labels, writer identities, or evaluation answers. All 50 responses match the executed state, and none flags ambiguity or reinstatement of an old value. This is model-based semantic validation. Calls use the native OpenAI, requested and returned identifier `gpt-6-astra`, high reasoning, and an 8,192-token cap. Scoring compares the complete normalized answer with current, old-target, unused-target, and other-field values. Appendix F.3 reports the paired results.

D.4 Decisions under revised constraints

This component asks models to use updated state to choose an action. The 24 evaluation scenarios comprise 12 procurement dialogues and 12 scheduling logs, separate from six development scenarios. Requirements can inherit shared defaults, override them locally, or withdraw earlier directives, and unmentioned fields persist. Procurement combines venue, catering, and shuttle choices, while scheduling combines room and time assignments. Fixed catalogues, explicit objectives, and tie rules define a unique optimal action. A ledger interpreter, independent reverse replay, and exhaustive action enumeration verify the labels before evaluation.

Each scenario crosses 24- or 96-directive histories, single or composed actions, and three context conditions: full history, resolved target state, and a word-count-padded resolved state. These produce 12 paired conditions per scenario (288 prompts per model). The snapshot supplies constraints, not the optimal action. Scoring records optimality, constraint satisfaction, and matches to historical or other-project optima, while invalid outputs, refusals, truncations, and provider failures remain separate. Appendix F.4 also reports small exploratory tool-provenance and negotiated-planning pilots, which are not counted among the 24 evaluation scenarios.

D.5 Dependent updates in operational histories

Warehouse-dispatch and build-release logs track 16 slots containing immutable identifiers. Each committed production handoff cycles the current contents of two, three, or four slots, while sandbox and aborted operations leave the state unchanged. A query requests the current identifier in one slot after 2,048 operations. The two settings share this state-transition system. Initial states and transition rules are supplied in the prompt, and every operation needed to compute the answer is present.

The confirmation cohort contains 40 fresh scenarios, 20 per setting, distinct from four development scenarios. Forward replay, inverse ancestry, and an independent parser of the rendered log verify each answer. Every full history is paired with a resolved-state snapshot, yielding 80 primary prompts. The snapshot is a solvability control that removes state reconstruction, but it is not matched for length or computation. Models answer through the API without executable tools or external memory. Scoring checks the requested identifier and records response availability separately. Full prompts and responses are retained in the reproducibility artifacts, and source-verified failure excerpts appear in Appendix F.5.

The deferred-log tier uses the same slots, surfaces, and cycle semantics with one additional rule: a handoff logged with `status=pending` does not execute at its own line and executes only when a later line `resolve(seq=N); result=committed` refers to it, on the contents current at that line, while `result=aborted` or the absence of a resolution cancels it, and sandbox operations never affect production. Lines are drawn with production probability 0.85, and statuses committed, aborted, and pending are drawn with probabilities 0.55, 0.15, and 0.30. Each pending operation is scheduled for resolution with probability 0.8 after a delay of 1–400 lines (dropped beyond the log end), with a committed result with probability 0.6. Resolve lines consume sequence numbers, so a 1,024-line log contains on average 166 resolve lines and 485 effective operations, 82 of which execute only through a resolution, and the queried item's dependency chain averages 92 operations. Each scenario has three conditions. The first is the deferred history. The second is a linearized control in which pending lines become aborted and each resolve line becomes the full committed or aborted handoff it stood for, so the effective operations and their line numbers are identical without cross-line dependency. The third is the resolved snapshot. The confirmation cohort has 40 scenarios and the development cohort 4, and forward simulation with an explicit pending table, an inverse trace over effective operations, and an independent parser of the rendered text verify every label, and the

linearized twin is verified to reproduce the same final state. Seventeen confirmation scenarios, fixed in index order before any answer, were evaluated within the inference budget.

D.6 Provenance and reproducibility

PrefEval supplies preference content for the original core. The extensions use newly constructed state ledgers, catalogues, and operational histories. Generation models supply dialogue wording, while executable rules determine answers. We retain the construction seeds, scenario and condition identities, programmatic labels, prompts, validation records, and raw evaluation responses. API records include requested and returned model identifiers, provider, collection date, and token usage. Repeated conditions remain linked to their underlying scenario for paired analysis, and development and confirmation cohorts are reported separately. The experiment code and CICM dataset are publicly available at `https://github.com/JamesJunyuGuo/CICM`.

E Test-time attention routing

We give the routing method, calibration, and controls behind Table 2.

E.1 Identifying and attending to the current assignment

The parser uses the dialogue, predefined variables and values, and tokenizer offsets. It identifies the queried variable from the final question and scans preceding user messages for updates. The latest valid update supplies the current value, and mentions of different values supply old-value positions. Reminders containing both "still thinking about" and "compare options" are not updates, and assistant messages do not set the current value. Saved answer labels and spans are used only to check the parser, not as its inputs. This grammar-specific parser could itself answer the direct question. The reminder baseline instead inserts its parsed value in an assistant message before the query and lets the model answer.

Equation 4 changes selected query heads only at the final prompt position, after native scaling, masking, and any softcapping, before softmax. Shared keys are first expanded to query heads in grouped-query attention. Later cached decoding steps are not directly modified, although effects can propagate. Weights, value vectors, and output logits are not directly overwritten.

For adaptive routing, let m be the calibrated target log-ratio of attention on current versus old positions. Using the sets C, O and scores s_j defined in Section 6, the existing log-ratio δ and the applied bias are

$$\delta = \log \sum_{j \in C} e^{s_j} - \log \sum_{j \in O} e^{s_j}, \qquad \beta = \min\left(8, \max\left(0, \frac{m - \delta}{2}\right)\right). \tag{18}$$

The softmax denominator cancels: the bias increases the attention log-ratio by 2β, reaching m unless capped. A sufficient ratio is left unchanged. This does not fix answer probabilities or the total attention on these positions relative to other context.

E.2 Calibration and held-out evaluation

The 1,200 CICM dialogues (Appendix D) cover three variables, seven values each, and six combinations of competitor distances. A deterministic identifier hash assigns 40 of each cell's 200 dialogues to calibration and 160 to testing. Adaptive calibration splits into 120 discovery and 120 validation dialogues. Variables, vocabulary, and templates are not held out.

With weights frozen, we differentiate the current-minus-strongest-old first-token answer score with respect to a gate on each head's intervention, at zero intervention ($m = 1$, bias cap 8). Scores combine tokenization variants by log-sum-exp. Heads are ranked by average gradient on discovery old-value errors. First-token collisions are excluded from this objective, not from full-response evaluation. The gradient measures local sensitivity, not each head's independent correction effect. Validation tests the highest-ranked positive-gradient heads in sets of size $1, 2, 4, 8, 16, 32$ with $m \in \{0.5, 1, 2, 4\}$. We maximize positive accuracy gain while preserving at least 95% of correct answers, breaking ties toward fewer heads and smaller m (frozen settings: Table 12).

Fixed-bias runs use eight heads and select $\beta \in \{0.5, 1, 2, 4, 8\}$ under the same preservation constraint, without separating discovery and validation. Qwen2.5-7B's eight heads are inherited from Stage B on the separate synthetic assignment dataset, and the saved frozen head list exactly matches that analysis, not the CICM attention comparison in Section 4. Qwen2.5-14B's are ranked on calibration data by the failed-minus-correct difference in log(old/current attention). Frozen configurations apply to every test dialogue regardless of baseline correctness.

Checkpoints are instruction-tuned, and decoding is greedy with bfloat16 weights and an eight-token limit. Runs use H100 GPUs and batch size 12. Inference uses one decode, no gradients, and eager attention.

E.3 Retrieval estimates and controls

Adaptive gains mainly correct old-value errors while preserving correct answers (Table 12). Value matching prioritizes current, old, unused same-variable, other-variable, then other text. This is not whole-string matching: answers containing both current and old values can count as correct. Counting all mixed-value answers as incorrect leaves Qwen, Llama-3.2-3B, and Gemma gains unchanged, while Llama-3.1-8B gains 46.82 points and Mistral 76.88 points under this stricter rule.

Main-text accuracies weight dialogues equally. For uncertainty, dialogues form 210 groups defined by variable, current value, overwrite count, and competitor distances. We average paired correctness differences within groups, then resample groups 2,000 times and average their means. These equally weighted group estimates can differ from dialogue-weighted gains, and intervals condition on the frozen configuration, excluding head-selection uncertainty.

Table 12: Frozen routing settings and held-out retrieval outcomes. Counts show old-value errors corrected and originally correct answers preserved. Gain is the equally weighted group estimate (percentage points), with its 95% bootstrap interval.

Model	Heads	Setting	Corrected	Preserved	Group gain [95% interval]
Qwen2.5-3B	32	$m = 4$	678/711	156/158	78.37 [74.51, 82.21]
Llama-3.2-3B	32	$m = 4$	514/541	266/266	64.60 [59.40, 69.63]
Llama-3.1-8B	16	$m = 4$	395/467	400/400	46.90 [41.99, 51.93]
Mistral-7B-v0.3	32	$m = 2$	564/674	51/52	75.01 [70.33, 79.12]
Gemma-2-9B	32	$m = 4$	407/455	452/452	45.06 [39.63, 50.99]
Qwen2.5-7B	8	$\beta = 8$	208/487	361/361	31.80 [27.88, 35.76]
Qwen2.5-14B	8	$\beta = 2$	13/491	383/389	1.17 [0.14, 2.24]

Targeted routing outperforms random controls, and reversing it harms accuracy (Table 13). We test 16 random-position sets matching positive/negative token counts and excluding controlled values. Adaptive runs also test 64 random-head sets matching counts per layer and excluding selected heads. They use the same rule, but adaptive biases can differ: these are not matched-norm controls. Reverse routing recomputes its bias in the opposite direction. The reminder comparison is descriptive, without a separate paired significance test against routing.

Table 13: Control gains in retrieval accuracy (percentage points). Random columns report means and empirical 95% ranges across sampled sets, not confidence intervals for paired effects. A dash means the control was not run.

Model	Random positions	Random heads	Reverse routing
Qwen2.5-3B	$0.08\ [-0.27, 0.38]$	$-9.98\ [-14.42, -1.28]$	-16.35
Llama-3.2-3B	$-0.17\ [-0.48, 0.07]$	$-5.05\ [-12.19, 0.88]$	-27.08
Llama-3.1-8B	$-0.36\ [-0.69, 0.00]$	$-2.52\ [-10.90, 3.05]$	-28.15
Mistral-7B-v0.3	$0.03\ [-0.10, 0.21]$	$-0.49\ [-1.50, 0.45]$	-3.65
Gemma-2-9B	$0.19\ [-0.07, 0.38]$	$-3.04\ [-7.07, 1.32]$	-27.71
Qwen2.5-7B	$0.15\ [-0.42, 0.59]$	—	-16.04
Qwen2.5-14B	$0.18\ [0.00, 0.38]$	—	-1.77

E.4 Diagnostic checks and interpretation

Gemma-2-9B increases accuracy from 47.08% to 91.88%, compared with 82.81% for the reminder, and preserves all 452 initially correct answers (Table 2).

Among 960 examples, routing led to a 44.79-point gain in accuracy, 407/455 old-value corrections, and 452/452 correct answers preserved. Thus the large Gemma gain persists in this sensitivity analysis.

These results support controllable selection, not unique heads or a shared native cause of errors. Calibration uses labels and gradients, while parsing uses structured update knowledge. Differing model versions and protocols preclude a scaling claim. Earlier alternatives were less successful: global per-head steering did not beat random directions, fixed attenuation selected no eligible nonzero change, and Qwen2.5-1.5B routing did not exceed the random-head range. They motivated the adaptive method but are not further replications.

F Behavioral robustness and task diversity

These behavioral checks examine the interpretation of later mentions, answer-generation settings, and broader update tasks. They use new API responses and frozen paired inputs. The original mechanism and routing estimates retain their original dialogues, and the checks below do not re-estimate those internal measurements on the modified prompts.

F.1 Paired CICM wording and placement tests

Design. For each of the original 1,200 dialogues, we compare five conditions. The first keeps the original wording. The second adds an explicitly historical reminder, "For the record, [value] was an earlier choice for my [slot], and is no longer current". The third replaces the old value with neutral text that retains its message position and whitespace word count. The fourth asks for the most recent explicit update and specifies that later mentions of earlier choices are not updates. The fifth combines the historical wording with the explicit question. The current assignment, other-variable updates, acknowledgments, and message count remain fixed. This yields 6,000 condition rows per model. In original far-old dialogues, the historical reminder and the neutral replacement are no-ops, and the combined condition is identical to the explicit question, so exact duplicate requests reuse the same response and are not independent trials.

The separate placement test uses the 600 original far-old dialogues. Both conditions contain the same explicitly historical old-value mention and explicit-update question. We swap that mention and its acknowledgment with a value-free filler pair, preserving the complete multiset of message contents and the exact positions of current and other-variable updates. The historical mention is 2–8 messages from the question in the near condition and 20–32 in the far condition. This produces 600 paired comparisons per model with equal mention counts, and unlike the original factorial, this contrast isolates placement from adding a reminder.

Execution and scoring. Qwen2.5-7B-Instruct and GPT-4o receive the same frozen conditions through OpenRouter with temperature zero and a 16-token output cap. A balanced screen covers 180 original dialogues and 90 placement pairs, and the full design, designated as primary before inspecting screen effect estimates, contains those items and is not a held-out replication. Identical cached responses are reused only after checking input and request hashes. We preserve returned model/provider metadata, token usage, raw responses, termination reasons, and retries.

The primary score matches the entire normalized final answer against the fixed value vocabulary, allowing an optional "Answer:" prefix. It does not count an explanation as correct merely because it mentions the gold value. This is a new evaluation, not a re-scoring of the original gold-anywhere results. Old-value rate denotes old responses divided by all valid responses, while old-value share of errors uses only incorrect responses as its denominator. Paired differences use the same source dialogues, and uncertainty conditions on these generated items. The stronger-model comparison measures task solvability under these labels. A separate blinded GPT-6 Astra review checks 50 generated-language extension dialogues (Appendix F.3), and this is model-based semantic validation.

Table 14: CICM wording and query ablations on the full source set. Each entry is current-value accuracy / old-value answer rate (%), with 600 dialogues per source condition.

	Qwen2.5-7B		GPT-4o	
Variant	Near source	Far source	Near source	Far source
Original	12.3 / 84.8	65.7 / 14.5	79.7 / 19.0	94.5 / 2.3
Explicit historical wording	62.5 / 25.5	65.7 / 14.5	98.5 / 0.0	94.5 / 2.3
Neutral replacement	62.3 / 17.0	65.7 / 14.5	95.0 / 2.8	94.5 / 2.3
Explicit-update query	7.3 / 87.3	61.2 / 9.8	88.7 / 8.8	94.8 / 1.7
Combined	39.2 / 41.8	61.2 / 9.8	99.3 / 0.0	94.8 / 1.7

Near and far refer to the original source conditions, pooled over update counts and other-variable distances. Old-value rates use all 600 dialogues as the denominator. Historical wording and neutral replacement leave far-source prompts unchanged; combined equals the explicit-query variant there. These are wording ablations, separate from the matched placement test below.

Wording matters, but does not account for all errors. All 14,400 condition rows have valid, untruncated responses, representing 10,800 distinct API requests after exact-prompt reuse. In the 600 near-source dialogues, historical wording raises Qwen accuracy from 74/600 to 375/600 (a paired gain of 50.2 points, 95% interval $[46.0, 54.3]$), and neutral replacement gives 374/600. The explicit-update question alone does not rescue Qwen: accuracy is 44/600, versus 235/600 with both treatments. GPT-4o scores 478/600 on original near-source prompts, 591/600 with historical wording, and 596/600 with both treatments (Table 14). The question-only rewrite instead improves GPT-4o to 532/600. Its effect is therefore model-dependent. One possible explanation for Qwen is that mentioning "earlier choices" in the clarification makes historical alternatives more salient, consistent with selection competition. The rewrite also changes update and slot instructions, so this lexical hypothesis is not isolated by the present comparison.

The originally showcased near-old/far-other cell contains 200 dialogues. On these same sources, Qwen returns old values in 190/200 original prompts, 59/200 with historical wording, and 45/200 with neutral replacement. GPT-4o scores 191/200 originally and 194/200 with historical wording, and the latter has no old-value answers. At $k = 1$, across the three near-source other-variable distances, Qwen accuracy rises from 27/120 to 96/120 under historical wording, and GPT-4o from 97/120 to 117/120. Thus the low original near-source baseline is sensitive to wording, while explicitly obsolete values can still be returned.

Table 15: Matched placement of an explicitly historical value. Each model answers 600 paired dialogues; the current update, other-variable updates, message count, and message-content multiset are fixed within a pair.

Model	Answer type	Far (%)	Near (%)	Difference
Qwen2.5-7B	Current value	58.8	46.7	-12.2
	Old value	14.8	36.7	+21.8
GPT-4o	Current value	98.3	96.5	−1.8
	Old value	0.0	0.0	0.0

Differences are near minus far. Intervals use 2,000 paired bootstrap resamples of source dialogues (seed 20260920). Both arms explicitly identify the repeated value as obsolete and ask for the latest explicit update. GPT-4o produces no old-value answers in either arm, yielding a degenerate empirical bootstrap interval; the Wilson upper endpoint for each 0/600 rate is 0.64%.

Equal-mention placement. In the separate matched test, Qwen returns old values on 89/600 far and 220/600 near prompts, a paired increase of 21.8 points (95% interval $[18.0, 25.8]$). Accuracy falls from 353/600 to 280/600: 66 pairs change from incorrect to correct and 139 from correct to incorrect. GPT-4o scores 590/600 and 579/600, respectively, with no old-value answers, and its 31 errors select another variable's value. The old-value placement effect therefore persists in Qwen under explicit update semantics, while the stronger model largely solves this controlled task.

Uncertainty and API provenance. Paired intervals use 2,000 source-dialogue bootstrap resamples, and they do not treat reused variant rows as independent observations. All Qwen requests return `qwen/qwen-2.5-7b-instruct` from Phala. GPT-4o requests return `openai/gpt-4o` through OpenAI or Azure. Restricting GPT near-source comparisons to pairs routed through the same provider gives historical, neutral, query-only, and combined accuracy gains of 17.8, 14.9, 7.8, and 15.3 points ($n = 304, 308, 295, 301$), versus 18.8, 15.3, 9.0, and 19.7 points on all 600 pairs. These are descriptive provider-subset checks, not randomized provider controls. Full counts by update load, distance cell, variant, and provider accompany the saved response-level records.

F.2 Output budget and concise reasoning

Design. We select 50 existing 80-line overwrite prompts at each $k \in \{2, 4, 8\}$, using a fixed content-hash ordering. Each receives a paired no-overwrite control: only earlier target-variable names change to fresh names of the same character length. Values, line positions, the final target assignment, and the query stay fixed. The confirmation set contains 150 overwrite/control pairs, disjoint from the 10 pairs used to check the pipeline.

Qwen2.5-7B-Instruct is evaluated with the original integer-only instruction at 16- and 512-token caps, and with a concise-reasoning instruction at the same 512-token cap: "Briefly identify the queried variable's most recent assignment. Use at most one sentence of reasoning, then end with exactly one line in the form `FINAL: <integer>`." These arms use temperature zero. Reasoning versus the long direct-answer arm compares the instruction at an equal output cap, while long versus short direct answers isolates the cap with the instruction unchanged.

Answer extraction. Direct answers must be a complete integer, allowing a terminal period. Reasoning answers must contain exactly one terminal `FINAL:` integer, and numbers elsewhere in the explanation are ignored. During the disjoint smoke check, five of 20 Qwen reasoning responses put this field on the same line as the explanation. Before any confirmation calls, we froze a parser that accepts this whitespace variation while rejecting multiple fields and trailing text. Original strict-line scores and raw responses remain archived, and strict-format sensitivity is reported separately. API failures and truncations are distinguished from incorrect completed answers. When a wrong value belongs both to an old target assignment and another variable, we retain an ambiguous error category rather than assigning it uniquely to old-value selection.

High-load operational-identifier updates. A separate frozen confirmation set contains 36 fresh scenarios across six domains (meeting rooms, delivery routes, storage bins, service desks, pickup lockers, and document trays) and scalar or partial-record updates. Fixed templates render 384 user–assistant pairs. The target receives k distinct old identifiers before its current value, and a later mention explicitly marks an old identifier as obsolete. No-overwrite controls replace earlier target writes with neutral text, while cross-record controls redirect them to another record and field. Corresponding messages match whitespace-word counts, although token counts can differ. The event ledger supplies current and old answer labels. Before confirmation we froze 36 bases, five loads $k \in \{4, 16, 64, 128, 256\}$, and scoring rules. Each setting comprises 540 condition rows and 396 unique prompts because identical controls share responses. Table 16 presents the highest-load endpoint, and the full grid and paired analyses remain in the experiment archive.

Qwen and GPT-4o use temperature zero with direct-32, direct-512, or concise reasoning-512 outputs. Concise reasoning requests at most one explanatory sentence and a terminal `FINAL:` identifier. GPT-5 and Gemini 3.1 Pro Preview use medium reasoning and 8,192-token caps, while DeepSeek V4 Pro 0813 uses high reasoning and 32,768 tokens. These API settings do not equate reasoning computation. Direct answers score the normalized full reply, while reasoning arms score the terminal identifier. Protocol failures and truncations are recorded separately. Fourteen Qwen rate-limited requests received one additional attempt under a frozen recovery protocol. All completed, and no task answer was retried. Exact request/model/provider metadata and all attempts are archived.

At $k = 256$, Qwen and GPT-4o each return 32/36 old values under concise reasoning. GPT-4o solves every paired control in all three output settings. GPT-5 and Gemini solve all tested loads through $k = 256$, while DeepSeek returns two old values at this endpoint. These results distinguish resistance to repeated explicit updates from performance on the dependent histories in Appendix F.5.

Table 16: High-load updates ($k = 256$): 36 frozen scenarios per setting. Controls report correct answers; overwrite columns distinguish current and old values.

Model	Output, token cap	Current	Old	No overwrite	Cross-record
Qwen2.5-7B	Direct, 32	0/36	36/36	34/36	36/36
Qwen2.5-7B	Direct, 512	0/36	36/36	34/36	36/36
Qwen2.5-7B	Concise, 512	0/36	32/36	36/36	33/36
GPT-4o	Direct, 32	3/36	31/36	36/36	36/36
GPT-4o	Direct, 512	3/36	32/36	36/36	36/36
GPT-4o	Concise, 512	4/36	32/36	36/36	36/36
GPT-5	Reasoning, 8,192	36/36	0/36	36/36	36/36
Gemini 3.1 Pro	Reasoning, 8,192	36/36	0/36	36/36	36/36
DeepSeek V4 Pro	Reasoning, 32,768	34/36	2/36	35/36	35/36

All requested prompts remain in the denominator. At this load, every overwrite response completes; remaining overwrite outcomes are other answers (Qwen concise: 4; GPT-4o direct-32: 2; direct-512: 1). DeepSeek's no-overwrite control has one unsuccessful provider finish; all other control errors are other answers.

F.3 Task and language diversity

This experiment tests whether old-value errors extend beyond the original preference templates. We evaluate 180 state ledgers spanning six domains and three update operations: single-value replacement, partial-record updates, and full-record replacement. Each ledger has four paired versions crossing template or model-generated language with near or far placement of the same explicitly obsolete mention. Within each placement pair, value-mention counts and the current assignment's position are fixed. The query explicitly asks for the state after all updates. Appendix D.3 gives the construction, generation models, and validation procedure.

Evaluation. Qwen2.5-7B-Instruct, Llama-3.1-8B-Instruct, and GPT-4o receive all 720 prompts through OpenRouter, with temperature zero and a 16-token output cap. All 2,160 responses complete without API errors or truncation. A frozen matcher compares the complete normalized answer with the program-derived state and separately identifies old target values and values of other fields. Intervals use 2,000 bootstrap resamples of whole ledgers within domain, update-load, and task strata, preserving the four paired versions.

Table 17: Old-value responses on generated CICM dialogues. Each placement contains the same 180 ledgers. The paired difference is near minus far in percentage points; brackets give 95% bootstrap intervals.

Model	Far	Near	Difference
Qwen2.5-7B	39/180 (21.7%)	50/180 (27.8%)	+6.1
Llama-3.1-8B	7/180 (3.9%)	5/180 (2.8%)	−1.1
GPT-4o	0/180 (0.0%)	0/180 (0.0%)	0.0

Core finding. Qwen returns old values across all six domains and all three operations. On generated language, moving the obsolete mention nearer the question increases its old-value rate by 6.1 percentage points (Table 17). The increase comes from record updates: old-value counts rise from 14 to 20 for partial records and from 11 to 19 for full replacement, while single-value counts fall from 14 to 11. Template language gives a similar pooled increase of 7.2%. Llama makes fewer errors and shows no pooled increase, and GPT-4o answers all 720 prompts correctly. Thus old-value selection extends beyond the original preference templates, while sensitivity to mention placement varies across models and update operations.

Scoring and provider checks. Accepting one Qwen field-prefixed answer changes its generated-language difference from 6.1 to 6.7 points. Accepting two Llama spelling variants raises its four-condition accuracy from 697/720 to 699/720 without changing old-value counts. Primary scores retain the frozen matcher. Qwen and GPT-4o have equal reported input-token counts within every placement pair. Llama uses several routed providers, and restricting generated-language pairs to

the 76 sharing a provider still yields no positive placement effect (-3.9%). These are descriptive sensitivity checks. Raw outputs, provider and token metadata, and task/domain breakdowns are retained in the reproducibility artifacts.

F.4 Updating constraints before making a decision

Task structure. We extend evaluation from current-field answers to decisions that depend on several updated constraints. Two constructed task families use executable ledgers and fixed language templates. In procurement dialogues, the assistant maintains requirements for six projects and books a venue, caterer, and shuttle. The components must agree on site and satisfy current capacity, accessibility, dietary, walking-distance, rating, and budget constraints. The objective is minimum total spend, with an explicit tie rule. A simpler query books only a venue from the same state and catalogue.

In scheduling logs, an agent arranges two sessions under current durations, attendance, equipment, room availability, shared-room, and break requirements. It minimizes the second session's finish time, then room cost and explicit secondary criteria. The simpler query schedules only the first session. The log includes successful cached planning proposals tied to the directives that produced them, and these are neither executed bookings nor new requirements. A changed constraint can invalidate a proposal without replacing its text. These are constructed dialogues and agent logs, not sampled deployment traces. Family and presentation covary, so their difference is not a surface-only test.

Scope and withdrawals. Each project inherits shared defaults until it has an active local override. Local overrides take precedence over later shared defaults. Within a scope, the latest active assignment to a field wins, and unmentioned fields persist. A withdrawal deactivates only its named earlier assignment, including every field that assignment changed. Remaining active directives determine the state, and withdrawals are never themselves withdrawn. These rules are stated explicitly in each task. A ledger interpreter supplies the resolved state, and independent reverse-lookup replay and enumeration check the optimal actions.

Context and task complexity. Each scenario has a 24-directive history and a paired 96-directive history that inserts 72 updates to other projects. The target's relevant directives, opaque references, current state, and catalogue remain fixed. Each history supports both a single-action and a composed-action query. Each query has three input conditions: full history, an explicit final target-state snapshot, and that snapshot padded to the history's whitespace-word count. The snapshots still require solving the decision problem and never supply its answer. Padding consists of repeated instances of the word "note", not natural distractor dialogue. It is therefore an artificial word-count control whose response pathologies must be distinguished from historical interference. Actual token counts are recorded rather than assumed equal. The longer-history contrast therefore changes contextual interference, not the number of target updates.

The development cohort contains six scenarios. A separate fixed seed generates 24 evaluation scenarios, 12 per family, with no development prompt overlap. There are 12 condition rows per scenario and 288 per model. Scenarios are constructed to have a feasible unique optimum under the stated tie rule and at least two distinct superseded optima during the relevant update history. This programmatic enrichment precedes model answers. All scenarios are retained, including models' successful cases. Identical snapshot requests may share a cached response when their scoring contracts also agree, and request identities track reuse and separate repeated calls. They are not additional independent scenarios.

Generation and scoring. GPT-5, Gemini 3.1 Pro Preview, DeepSeek V4 Pro 0813, and Claude Sonnet 5 use high reasoning effort. DeepSeek has a 32,768-token completion cap and the other models have 16,384, and these settings do not equate computation across families. The final answer specifies component identifiers or room/time pairs, composing an action rather than selecting a prewritten complete answer. Transport failures receive at most two retries, and answer outcomes are never selectively retried.

A development-only formatting check shows that some models surround a correct identifier with a short booking phrase. Before evaluation, we freeze a conservative terminal-action parser that accepts identifiers, role labels, punctuation, and a booking phrase naming the correct project. It rejects

negation, alternatives, conflicting projects, excess identifiers or times, and missing terminal answers. All original strict-format scores are retained. Refused and truncated responses remain separate from semantic errors.

Primary accuracy is the probability of returning the current optimal action per requested prompt. We also report satisfaction of all current hard constraints, feasible but nonoptimal decisions, and matches to a superseded or another project's optimum. A historical-optimum match is consistent with obsolete constraints, but it does not establish which information caused the answer or transfer the open-model circuit diagnosis. The primary paired comparison is composed-task accuracy under long history minus its padded snapshot control. Supporting comparisons vary task complexity and contextual load. Intervals use 2,000 bootstrap resamples of whole scenarios within family, retaining all 12 conditions together.

Decisions remain largely correct under full history. Tables 18–20 give all task, context, and control cells. Under full history, optimal answers per requested prompt are GPT-5 92/96, Gemini 95/96, DeepSeek 92/96, Sonnet 88/96. Every action accepted by the frozen parser in these history conditions is optimal, and the remaining outcomes are invalid terminal outputs, provider failures, or truncations, rather than interpretable nonoptimal actions. Four GPT-5 history answers identify the correct venue but add an unrequested date or wording outside the frozen grammar. Their primary scores remain invalid-output outcomes, and they are not evidence of obsolete-state use.

Gemini's three interpretable decision errors all occur in the long, composed procurement task with the padded current-state control: two actions violate current constraints and one is feasible but nonoptimal. One infeasible action matches a historical optimum even though that input contains no history. Such a match alone therefore cannot diagnose use of an obsolete state in a composed-action task. The repeated-word control also produces invalid outputs and truncations. Positive history-minus-padding differences cannot be interpreted as a benefit of historical interference. These tasks extend the tested action structure, but the observed history conditions do not show a semantic decision-failure effect in the reasoning models. The compact and padded controls, complete failure classes, and small number of independent scenarios delimit this result.

Requested model identifiers are `openai/gpt-5`, `google/gemini-3.1-pro-preview`, `deepseek/deepseek-v4-pro-0813`, and `anthropic/claude-sonnet-5`. Returned identifiers, providers, token usage and every attempt are retained.

Exploratory extensions with explicit dependencies. Two additional task-development pilots test structures absent from the initial families. A coding-agent pilot has 16 dependent tools, 18 versioned files, and two branches. A successful cached result is reusable only if its captured file versions and every recursively captured input artifact remain valid for the target branch. Late completion does not refresh captured inputs, and a newer stale result does not erase an older valid cache. The task requests the minimum set of tools to rerun. Six constructed scenarios have both full-history and current-files-plus-cache-input conditions, and the latter supplies neither freshness labels nor the execution plan. With high reasoning and a 16,384-token cap, GPT-5 and Gemini each recover all six minimum plans in both conditions. GPT-5 sometimes omits the "T" prefix from tool identifiers. An explicitly post-hoc equivalence check maps unique bare integers to the fixed tool list, and the original strict scores are retained, and these formatting differences are not missing steps.

A subsequent procurement pilot makes decisions jointly dependent through five supplier roles, ten incompatible pairs, and 30 stackable conditional credits. The objective is maximum total quality under the updated global budget, then minimum net cost and a stated identifier tie rule. Three scenarios are selected programmatically before answers: each has at least 15 feasible plans, its quality optimum differs from its cheapest plan, and credits enable strictly higher quality than any no-credit plan. Each has single-venue and composed-plan queries, with full history and explicit current-state controls. GPT-5 returns 11/12 optimal answers, and the remaining composed-history request reaches its 16,384-token cap, while its paired snapshot is correct. Gemini returns 12/12 optimal answers. Every completed plan is optimal. These adaptive exploratory pilots identify task structures and resource demands, but they do not establish a reliable frontier-model old-state failure. Their compact controls are not length-matched, and the small samples do not estimate deployment prevalence.

Table 18: Procurement dialogues: all 12 scenarios per cell. H denotes full history, S an explicit final-state snapshot, and P its word-count-matched padded version. Optimality counts successes per requested prompt. Unavailable includes invalid terminal output, provider failure/refusal, and truncation; it is separate from an infeasible or nonoptimal action. All interpretable history actions are optimal.

Context	Task	Optimal H / S / P	Unavailable H / S / P
GPT-5			
24 directives	Single	11 / 12 / 12	1 / 0 / 0
24 directives	Composed	12 / 12 / 12	0 / 0 / 0
96 directives	Single	9 / 12 / 12	3 / 0 / 0
96 directives	Composed	12 / 12 / 12	0 / 0 / 0
Gemini 3.1 Pro Preview			
24 directives	Single	12 / 12 / 12	0 / 0 / 0
24 directives	Composed	11 / 12 / 12	1 / 0 / 0
96 directives	Single	12 / 12 / 1	0 / 0 / 11
96 directives	Composed	12 / 12 / 1	0 / 0 / 8
DeepSeek V4 Pro 0813			
24 directives	Single	12 / 12 / 12	0 / 0 / 0
24 directives	Composed	12 / 12 / 12	0 / 0 / 0
96 directives	Single	11 / 12 / 12	1 / 0 / 0
96 directives	Composed	12 / 12 / 12	0 / 0 / 0
Claude Sonnet 5			
24 directives	Single	10 / 12 / 12	2 / 0 / 0
24 directives	Composed	10 / 12 / 12	2 / 0 / 0
96 directives	Single	10 / 12 / 11	2 / 0 / 1
96 directives	Composed	12 / 12 / 7	0 / 0 / 5

Table 19: Scheduling agent logs: all 12 scenarios per cell. H denotes full history, S an explicit final-state snapshot, and P its word-count-matched padded version. Optimality counts successes per requested prompt. Unavailable includes invalid terminal output, provider failure/refusal, and truncation; it is separate from an infeasible or nonoptimal action. All interpretable history actions are optimal.

Context	Task	Optimal H / S / P	Unavailable H / S / P
GPT-5			
24 directives	Single	12 / 12 / 12	0 / 0 / 0
24 directives	Composed	12 / 12 / 12	0 / 0 / 0
96 directives	Single	12 / 12 / 12	0 / 0 / 0
96 directives	Composed	12 / 12 / 12	0 / 0 / 0
Gemini 3.1 Pro Preview			
24 directives	Single	12 / 12 / 12	0 / 0 / 0
24 directives	Composed	12 / 12 / 12	0 / 0 / 0
96 directives	Single	12 / 12 / 11	0 / 0 / 1
96 directives	Composed	12 / 12 / 11	0 / 0 / 1
DeepSeek V4 Pro 0813			
24 directives	Single	11 / 12 / 12	1 / 0 / 0
24 directives	Composed	10 / 11 / 12	2 / 1 / 0
96 directives	Single	12 / 12 / 12	0 / 0 / 0
96 directives	Composed	12 / 12 / 12	0 / 0 / 0
Claude Sonnet 5			
24 directives	Single	11 / 12 / 12	1 / 0 / 0
24 directives	Composed	12 / 12 / 12	0 / 0 / 0
96 directives	Single	11 / 12 / 12	1 / 0 / 0
96 directives	Composed	12 / 12 / 12	0 / 0 / 0

Table 20: Paired optimal-action differences on 24 scenarios (percentage points, 95% whole-scenario bootstrap intervals). H, S, and P are defined above. The first two columns use the 96-directive composed task; the final column subtracts the single-task H−P difference from the composed-task H−P difference at that length. All-requested denominators retain no-answer outcomes.

Model	H − P	H − S	Change with composition
GPT-5	0.0 [0.0, 0.0]	0.0 [0.0, 0.0]	12.5 [0.0, 25.0]
Gemini 3.1 Pro Preview	50.0 [37.5, 62.5]	0.0 [0.0, 0.0]	0.0 [-16.7, 16.7]
DeepSeek V4 Pro 0813	0.0 [0.0, 0.0]	0.0 [0.0, 0.0]	4.2 [0.0, 12.5]
Claude Sonnet 5	20.8 [8.3, 33.3]	0.0 [0.0, 0.0]	29.2 [12.5, 50.0]

F.5 Frontier state reconstruction on complex operational histories

From overwrites to dependent state updates. We test frontier reasoning on current-state reconstruction through long sequences of dependent operations. Constructed warehouse-dispatch and build-release logs contain 16 slots holding immutable parcel or artifact identifiers. A handoff atomically cycles the *current* contents of two, three, or four slots, and the result of one operation becomes the input to later operations. Only committed production operations affect the queried state, while sandbox and aborted operations do not. The prompt supplies these rules, the initial state, all 2,048 operations in execution order, and a query for the single identifier to dispatch from one slot. There are no hidden updates. This uses permutation composition, an established state-tracking model system (Li et al., 2025), in two operational settings sharing the same transition rules.

Protocol. Task development used four pilot scenarios. Before collecting confirmation answers, we froze 40 fresh scenarios, each paired with a programmatically resolved current-state snapshot. All scenarios are included. Forward replay, inverse ancestry, and an independent parser of the rendered log verify the answers. We evaluate the model directly through the API, without executable tools, external memory, or a context-management harness. The snapshot is a separate solvability control: it supplies the final slot contents and removes the need to reconstruct them from history. It is not matched for length or computation, and does not evaluate a learned or deployed harness. Claude models were evaluated later on the identical frozen prompts through the native Anthropic API (official SDK, adaptive thinking, 128,000-token output cap, no tools).

Frontier reasoning models fail on full histories. GPT-5.6 Sol with high reasoning answers 9/40 full-history queries correctly, compared with 40/40 paired snapshots (Table 21). All 80 requests yield completed semantic answers, and none is truncated, refused, invalid, or lost to a provider error. Claude Opus 4.8 answers 18/40 correctly: 13 answers name an old occupant of the queried slot and 9 responses stop at the 128,000-token output cap without an answer. Among completed answers, accuracy is 18/31 (58.1%, Wilson [40.8, 73.6]%). Its 40 paired snapshots are all correct. Claude Sonnet 5 stops at the output cap on every pilot history (0/4 completed, snapshots 4/4), and its summarized reasoning describes a forward simulation of all sixteen slots that reaches only part of the log, so its outcome is an output-availability result, not a semantic one, and no confirmation was run. These are failures to identify the current operational state despite having the complete history and explicit transition rules. The contrast shows that using a supplied current state is substantially easier than reconstructing it through these updates.

Dependency-aware logs. To separate cross-line dependency from raw length, a second tier keeps the same state machine and surfaces but logs some handoffs as `pending`: such an operation executes only when a later line `resolve(seq=N); result=committed` refers to it, on the slot contents current at that line, while `result=aborted` or no resolution cancels it. Each 1,024-line scenario has three conditions: the deferred history, a linearized control with the identical effective operation sequence at the identical line numbers but every effect stated on its own line, and the resolved snapshot (construction in Appendix D.5). Opus 4.8 was evaluated on a pre-specified prefix of 17 of 40 frozen scenarios (Table 22): 12/17 deferred histories are correct against 16/17 linearized controls and 17/17 snapshots, with no truncation, and five scenarios fail only in the deferred form and one only in the linearized form (exact McNemar $p = 0.22$). Four separate development scenarios give 2/4, 4/4,

Table 21: Current-state accuracy on complex operational histories. The primary panels use the same 40 fresh paired scenarios, and brackets give Wilson 95% intervals over all requests. Truncation at the output cap counts as no answer. The exploratory panel reuses four separate pilot scenarios and is reported as counts. Sol and DeepSeek use high reasoning.

Model and cohort	Full history	Current-state snapshot
GPT-5.6 Sol, confirmation	9/40	40/40
Accuracy [95% interval]	22.5% [12.3, 37.5]	100% [91.2, 100]
Claude Opus 4.8, confirmation	18/40 (9 truncated)	40/40
Accuracy [95% interval]	45.0% [30.7, 60.2]	100% [91.2, 100]
Completed-answer accuracy	18/31 (58.1%)	40/40 (100%)
GPT-5.6 Sol, exploratory	0/4	4/4
DeepSeek V4 Pro 0813, exploratory	2/4	4/4
Claude Opus 4.8, exploratory	0/4	4/4
Claude Sonnet 5, exploratory	0/4 (4 truncated)	4/4

and 4/4. Every error names an old occupant of the queried slot. The remaining 23 frozen scenarios were not requested, and this exploratory comparison reports the complete pre-specified prefix.

Table 22: Dependency-aware logs: Claude Opus 4.8 on 1,024-line scenarios with pending operations resolved by later lines. The linearized control has the same effective operations at the same line numbers without cross-line dependency, and brackets give Wilson 95% intervals.

Cohort	Deferred history	Linearized control	Snapshot
Confirmation prefix (17 scenarios)	12/17	16/17	17/17
Accuracy [95% interval]	70.6% [46.9, 86.7]	94.1% [73.0, 99.0]	100% [81.6, 100]
Development (4 scenarios)	2/4	4/4	4/4

Settings and supporting checks. Sol uses OpenRouter model `openai/gpt-5.6-sol`, fixed provider OpenAI, high reasoning, and a 128,000-token output cap. Its longest confirmation completion is 34,918 tokens, and maximum input length is 51,836 tokens. Claude models use the native Anthropic API with returned identifiers `claude-opus-4-8` and `claude-sonnet-5`, adaptive thinking with summarized display, a 128,000-token output cap, and no sampling parameters, and history prompts are 67,181–67,359 Anthropic tokens. Completed Opus answers use 35,631–103,140 output tokens (median 43,778), and all 31 state a backward trace of the queried slot, while six of the nine truncated responses instead begin a full forward simulation of all sixteen slots. Thinking summaries are stored but never scored. The exploratory DeepSeek panel uses `deepseek/deepseek-v4-pro-0813`, fixed provider Wafer, high reasoning, temperature zero, and a 262,144-token cap. Sol and DeepSeek pilot answers complete normally. On those four pilot scenarios, Sol and DeepSeek each answer 4/4 correctly when every commit is cancelled and 4/4 when an accurate checkpoint is inserted before the final 512 operations. For Sol, cancelling commits preserves input bytes and token counts, and the checkpoint retains the earlier log and adds 147 tokens. Sol also answers 4/4 when irrelevant operations are removed and 4/4 when they are cancelled while preserving the complete necessary update chain. These are exploratory diagnostics on reused cases. A corresponding 40-scenario relevance study is incomplete: 8/40 compact and 10/40 masked requests returned, all correctly, before service-credit exhaustion. The other 62 outcomes are unavailable and contribute no accuracy estimate, and no completed recovery result is included here.

Auditable failure examples. Figures 8 and 9 show Sol's first failed confirmation scenario by index in each setting, and Figures 10 and 11 show Opus 4.8's first failed build-release scenario on the 2,048-operation tier and its first failed warehouse scenario on the dependency-aware tier, selected by the same rule. Input and answer excerpts are verbatim, apart from line wrapping and explicitly marked omissions. The model received all 16 initial entries and the complete log: 2,048 operations in the primary tier or 1,024 lines in the deferred tier. Green boxes contain post-hoc programmatic checks, which were not supplied in the full-history condition. The violet boxes reproduce visible

answers, not hidden reasoning traces. Full prompts, responses, model/provider metadata, and input hashes are retained with the reproducibility artifacts.

Warehouse dispatch — handoff_0000

Task rules (summary). Move current slot contents simultaneously around each listed cycle. Only committed production operations change state.

Initial production slots (excerpt).
`S08: P2070`
`S11: P6443`
[Other initial entries and earlier log entries omitted.]

Execution log (excerpt).
```
2037 handoff(cycle=[S01, S09, S08, S15]);
branch=sandbox; status=committed
```
[Intervening entries omitted.]
```
2041 handoff(cycle=[S11, S01, S07, S12]);
branch=production; status=committed
2042 handoff(cycle=[S10, S09, S13, S01]);
branch=production; status=committed
```
[Entries 2043–2048 omitted.]

Query (verbatim). The next dispatch must use the item currently in S01. Which P identifier should the agent dispatch? Reason as needed. End with exactly one line in the form FINAL: ¡one requested P identifier¿.

Sol answer to the complete history (verbatim)

Tracing S01 backward through committed production cycles leads to initial slot S11, which held P6443. FINAL: P6443

Verified current state (post-hoc annotation)

Immediately before operation 2042, `S13` contains `P2070`. That committed production handoff moves it to `S01`; no later committed production operation changes this slot. Full inverse replay traces `S01` to initial `S08`, not `S11`. The correct dispatch is **`P2070`**.

Figure 8: Warehouse dispatch failure with high reasoning. The model receives the complete history and returns an incorrect dispatch identifier. Selected log entries and the verified final transition explain the task; omitted entries remain part of the evaluated input. The paired snapshot answer is correct.

Build-release agent — handoff_0001

Task rules (summary). Move current slot contents simultaneously around each listed cycle. Only committed production operations change state.

Initial production slots (excerpt).

```
S01:  P1740
S03:  P6022
```

[Other initial entries and earlier log entries omitted.]

Execution log (excerpt).

```
2046 handoff(cycle=[S09, S11, S15]);
branch=production; status=committed
2047 handoff(cycle=[S07, S16, S06]);
branch=production; status=committed
2048 handoff(cycle=[S04, S11, S06]);
branch=sandbox; status=committed
```

Query (verbatim). The next dispatch must use the item currently in S11. Which P identifier should the agent dispatch? Reason as needed. End with exactly one line in the form FINAL: ¡one requested P identifier¿.

Sol answer to the complete history (verbatim)

Reverse-tracing S11 through only committed production cycles leads to initial slot S03, containing P6022.
FINAL: P6022

Verified current state (post-hoc annotation)

Immediately before operation 2046, `S09` contains `P1740`. That committed production handoff moves it to `S11`; no later committed production operation changes this slot. Full inverse replay traces `S11` to initial `S01`, not `S03`. The correct dispatch is **`P1740`**. Operation 2048 is a sandbox operation and leaves production unchanged.

Figure 9: Build-release agent failure with high reasoning. The model receives the complete history and returns an incorrect dispatch identifier. Selected log entries and the verified final transition explain the task; omitted entries remain part of the evaluated input. The paired snapshot answer is correct.

Build-release agent — handoff_0019

Task rules (summary). Move current slot contents simultaneously around each listed cycle. Only committed production operations change state.

Initial production slots (excerpt).

```
S11:  P4052
S16:  P7085
```

[Other initial entries and earlier log entries omitted.]

Execution log (excerpt).

```
0514 handoff(cycle=[S06, S11, S14, S08]);
branch=production; status=committed
```

[Intervening entries omitted.]

```
2044 handoff(cycle=[S05, S01, S15, S12]);
branch=production; status=committed
2045 handoff(cycle=[S11, S14, S04, S15]);
branch=production; status=committed
2046 handoff(cycle=[S04, S06, S12, S10]);
branch=production; status=aborted
2047 handoff(cycle=[S01, S03, S06, S13]);
branch=production; status=committed
2048 handoff(cycle=[S14, S09]);
branch=production; status=committed
```

Query (verbatim). The next dispatch must use the item currently in S01. Which P identifier should the agent dispatch? Reason as needed. End with exactly one line in the form FINAL: ¡one requested P identifier¿.

Opus 4.8 answer to the complete history (final lines, verbatim)

[3320 characters of the model's stated trace omitted; the full answer is in the raw record.]
After op 0003, target = S16, and no earlier committed production op touches S16.
The initial content of S16 is P7085.
FINAL: P7085

Verified current state (post-hoc annotation)

Immediately before line 2047, `S13` contains `P4052`. That committed production handoff moves it to `S01`; no later committed production operation changes this slot. Full inverse replay traces `S01` to initial `S11`, not `S16`. The correct dispatch is **`P4052`**. The answered identifier `P7085` last left `S01` at line 2044. The model's stated backward trace matches the verified chain for its 210 most recent transitions; at operation 514 (`handoff(cycle=[S06, S11, S14, S08])`) the tracked slot is `S08`, whose predecessor in the cycle is `S14`, but the trace moves to `S08`.

Figure 10: Build-release agent failure (Opus 4.8, high effort, 40-scenario confirmation). The model receives the complete history and returns an incorrect dispatch identifier. Selected log entries and the verified transitions explain the task; omitted entries remain part of the evaluated input. The paired snapshot answer is correct.

Warehouse dispatch — deferred_0002

Task rules (summary). Move current slot contents simultaneously around each listed cycle. Only committed production operations change state. A `pending` operation executes only when a later `resolve(seq=N); result=committed` line refers to it, on the contents current at that line.

Initial production slots (excerpt).

```
S02:  P7238
S07:  P7888
```

[Other initial entries and earlier log entries omitted.]

Execution log (excerpt).

```
0876 handoff(cycle=[S08, S09, S14, S12]);
branch=production; status=pending
```

[Intervening entries omitted.]

```
1004 handoff(cycle=[S07, S01, S15]);
branch=production; status=committed
1005 handoff(cycle=[S13, S14]);
branch=production; status=committed
1006 handoff(cycle=[S01, S07]);
branch=production; status=pending
1007 resolve(seq=0876); result=committed
1008 handoff(cycle=[S05, S08, S13]);
branch=production; status=pending
1009 handoff(cycle=[S16, S08]);
branch=production; status=pending
1010 handoff(cycle=[S02, S09, S07]);
branch=production; status=pending
```

[Entries after the excerpt omitted (14).]

Query (verbatim). The next dispatch must use the item currently in S14. Which P identifier should the agent dispatch? Reason as needed. End with exactly one line in the form FINAL: ¡one requested P identifier¿.

Opus 4.8 answer to the complete history (final lines, verbatim)

[477 characters of the model's stated trace omitted; the full answer is in the raw record.]
Checking all subsequent executing operations (lines 0008–1024): none of the committed operations or committed resolutions after that point touch S14 (line 1021's '[S10,S14,S12,S02]' remained pending and was never resolved).
Therefore S14 currently holds P7888.
FINAL: P7888

Verified current state (post-hoc annotation)

Immediately before line 1007, `S09` contains `P7238`. Line 1007 resolves the pending production handoff 0876 (`handoff(cycle=[S08, S09, S14, S12])`) as committed, which executes at that line and moves it to `S14`; no later executed operation changes this slot. Full inverse replay traces `S14` to initial `S02`. The correct dispatch is **`P7238`**. The answered identifier `P7888` last left `S14` at line 848.

Figure 11: Warehouse dispatch failure (Opus 4.8, high effort, deferred-log tier, 17-scenario prefix). The model receives the complete history and returns an incorrect dispatch identifier. Selected log entries and the verified transitions explain the task; omitted entries remain part of the evaluated input. The paired snapshot answer is correct.